

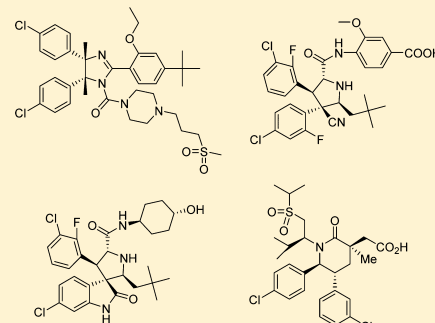
# Small-Molecule Inhibitors of the MDM2–p53 Protein–Protein Interaction (MDM2 Inhibitors) in Clinical Trials for Cancer Treatment

## Miniperspective

Yujun Zhao, Angelo Aguilar, Denzil Bernard, and Shaomeng Wang\*

University of Michigan Comprehensive Cancer Center and Departments of Internal Medicine, Pharmacology, and Medicinal Chemistry, University of Michigan, Ann Arbor, Michigan 48109, United States

**ABSTRACT:** Design of small-molecule inhibitors (MDM2 inhibitors) to block the MDM2–p53 protein–protein interaction has been pursued as a new cancer therapeutic strategy. In recent years, potent, selective, and efficacious MDM2 inhibitors have been successfully obtained and seven such compounds have been advanced into early phase clinical trials for the treatment of human cancers. Here, we review the design, synthesis, properties, preclinical, and clinical studies of these clinical-stage MDM2 inhibitors.



Representative MDM2 inhibitors in Clinical Development

## 1. INTRODUCTION

### 1.1. Interplay between Tumor Suppressor p53 and Its Negative Regulator MDM2.

The transcription factor p53 plays vital roles in the regulation of cellular processes and suppression of tumor development.<sup>1–5</sup> Mice lacking p53 develop normally but are prone to the development of a variety of tumors.<sup>6</sup> TP53, the gene encoding the p53 protein, is mutated or deleted in nearly 50% of human cancers, rendering p53 nonfunctional as a tumor suppressor.<sup>7</sup> Although p53 retains wild-type status in the remaining 50% of human cancers, its function is effectively inhibited by a variety of mechanisms. One major inhibitory mechanism is through overexpression of MDM2 (also called HDM2 in humans). The role of MDM2 as a primary negative endogenous regulator of p53 is supported by evidence that *MDM2*-null is embryonically lethal in mice which can only be rescued by concurrent deletion of the *TP53* gene.<sup>8,9</sup>

In cells, MDM2 and p53 regulate each other mutually through the autoregulatory feedback loop shown in Figure 1.<sup>10,11</sup> The autoregulatory feedback loop of the p53–MDM2 interplay operates as follows: upon activation, p53 transcribes MDM2, leading to an increase of MDM2 mRNA and protein and in turn, MDM2 protein binds to p53 directly through their N-termini and inhibits p53 function through three major mechanisms: (1) upon binding, MDM2 ubiquitinates p53 by functioning as an E3 ligase promoting proteasomal degradation of p53; (2) interaction of MDM2 with p53 blocks the binding of p53 to its targeted DNA, rendering p53 ineffective as a transcription factor; (3) MDM2 promotes export of p53 out of the cell nucleus, leaving p53 inaccessible to targeted DNA and reducing its transcriptional ability.<sup>10–12</sup> Through these three

inhibitory mechanisms, MDM2 functions as an effective antagonist of wild-type p53.

Consistent with its role as an efficient inhibitor of p53 tumor suppressor, MDM2 in cells, when overexpressed, is oncogenic.<sup>13</sup> An analysis of 28 different types of cancers involving nearly 4000 human tumor samples shows that in 7% of human cancers, the *MDM2* gene has been amplified.<sup>14</sup> In addition to MDM2 gene amplification, MDM2 overexpression can be caused by a variety of mechanisms, such as single nucleotide polymorphism at nucleotide 309 (SNP309) in its gene promoter, enhanced transcription, or increased translation.<sup>15–18</sup>

MDM2 overexpression correlates with poor clinical prognosis and poor response to current cancer therapies.<sup>15–18</sup> In supporting its powerful inhibitory role of p53 tumor suppressor function, MDM2 gene amplification and *TP53* gene mutation are mutually exclusive in human cancers.<sup>19,20</sup>

### 1.2. Targeting the MDM2–p53 Interaction as a New Cancer Therapeutic Strategy.

Because MDM2 plays a primary role in inhibition of the p53 tumor suppressor function and antagonizes p53 through their direct interaction, blockade of the MDM2–p53 protein–protein interaction would liberate p53 from MDM2, thus restoring the tumor suppressor function of wild-type p53. Agents designed to block the MDM2–p53 interaction may have a therapeutic potential for the treatment of human cancers retaining wild-type p53.

The MDM2–p53 interaction has been mapped to the first ~120 N-terminal amino acid residues of MDM2 and the first 30 N-terminal residues of p53.<sup>17,18</sup> In 1996, a high-resolution

Received: July 18, 2014

Published: November 14, 2014

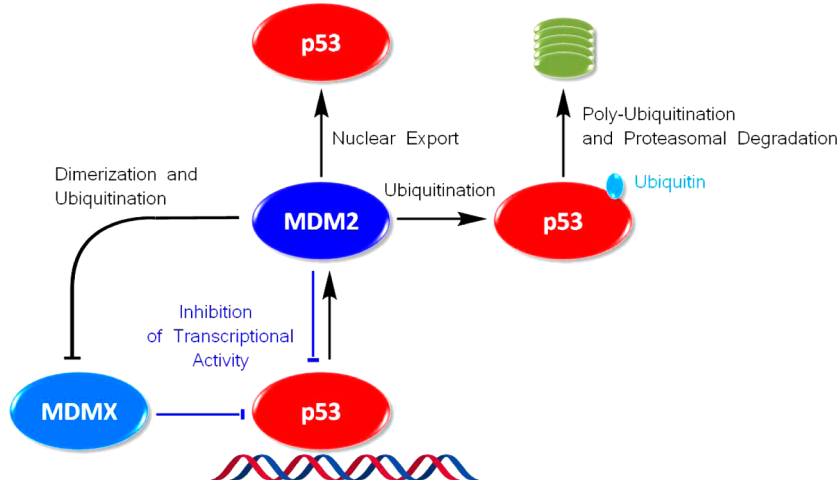


**Figure 1.** Inhibition of p53 by MDM2 and MDMX.

cocrystal structure of MDM2 with a p53 peptide (residues 15–29) was reported (Figure 2, PDB code 1YCR).<sup>21</sup> The cocrystal

clinical trials and discuss the outlook of MDM2 inhibitors as a new class of anticancer agents.

## 2. MDM2 INHIBITORS IN CLINICAL TRIALS FOR TREATMENT OF HUMAN CANCER

Currently, seven small molecule MDM2 inhibitors have advanced into clinical trials for treatment of human cancers (Table 1). Of these clinical-stage compounds, the chemical structures for RG7112 (3),<sup>31,32</sup> RG7388 (6),<sup>33,34</sup> MI-77301/SAR405838 (10),<sup>35,36</sup> and AMG 232 (14)<sup>37,38</sup> have been disclosed but no structural information is available for the other three compounds.

**2.1. RG7112.** **2.1.1. Discovery and Optimization.** The first MDM2 inhibitor to enter phase I clinical trials was 3 (Figure 3), discovered at Hoffmann-La Roche and based on a class of compounds called nutlins (Figure 3).<sup>39</sup>

In 2004, *cis*-diphenyl substituted imidazoline-containing compounds, called the “nutlins”, were reported as a first class of potent, specific, and orally active small molecule MDM2 inhibitors.<sup>39</sup> One of the most potent compounds in the initial report was nutlin 3a (1), which binds to MDM2 protein with  $IC_{50} = 90$  nM. A cocrystal structure of MDM2 complexed with nutlin 2<sup>39</sup> (2, Figure 4, PDB code 1RV1) was obtained at a resolution of 2.3 Å, which provided for the first time structural information for a non-peptide, small-molecule inhibitor bound to MDM2. Superimposition of the cocrystal structures of MDM2/2 and MDM2/p53 peptide (Figure 4) shows that two 4-bromophenyl rings and ethoxy substituent of 2 occupy the Trp23, Leu26, and Phe19 pockets of MDM2, respectively. This study provides an elegant example of a non-peptide, druglike, small molecule mimicking the  $\alpha$ -helical p53 peptide structure in its binding to MDM2.

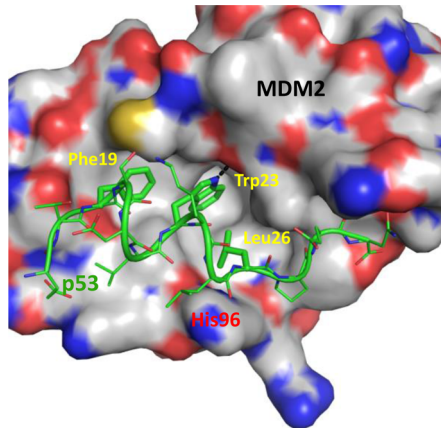


**Figure 2.** MDM2 (surface)–p53 (green line and sticks) complex.

structure showed that the MDM2-bound p53 peptide adopts an  $\alpha$ -helical conformation and interacts with MDM2 primarily through three hydrophobic residues, Phe19, Trp23, and Leu26. In this review, these p53 binding pockets on the MDM2 surface will be referred to as the Phe19, Trp23, and Leu26 pockets. These three p53 binding pockets in MDM2 are compact and well-defined and suggest the feasibility of the design of high-affinity, non-peptide inhibitors that bind in the MDM2 pockets (MDM2 inhibitors) and block the MDM2–p53 interaction.

Several reviews have summarized the progress in the design of MDM2 inhibitors.<sup>1,5,22–30</sup> In this review, we will focus on those MDM2 inhibitors that have been advanced into human

**Table 1. MDM2 Inhibitors in Human Clinical Trials for Cancer Treatments**

compd	clinical trial phase	originator	developer	ref
3 (RO5045337)	phase I	Roche	Roche	31, 32
6 (RO5503781)	phase I	Roche	Roche	33, 34
14	phase I	Amgen	Amgen	37, 38
CGM097	phase I	Novartis	Novartis	53
DS-3032b	phase I	Daiichi Sankyo	Daiichi Sankyo	54
10 (SAR405838)	phase I	University of Michigan	Sanofi S.A.	35, 36
MK-8242 (SCH 900242)	phase I	Merck	Merck	51

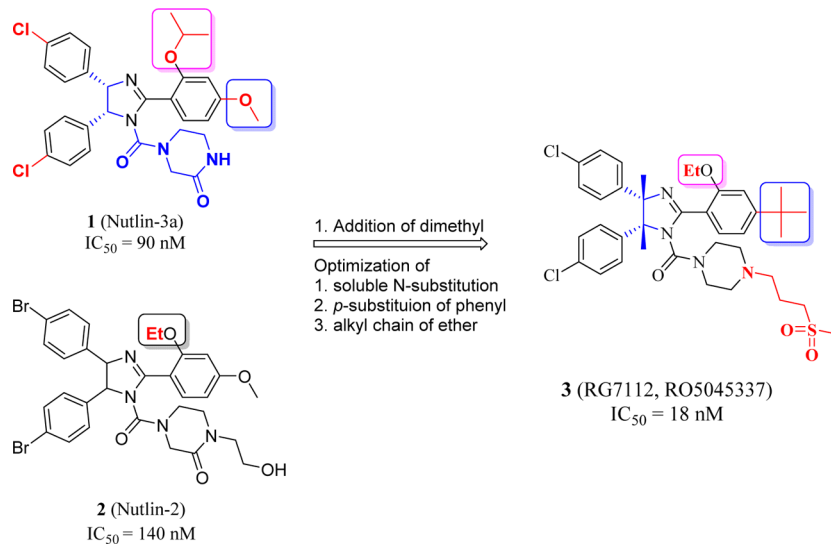


Figure 3. Nutlins and their analogs.

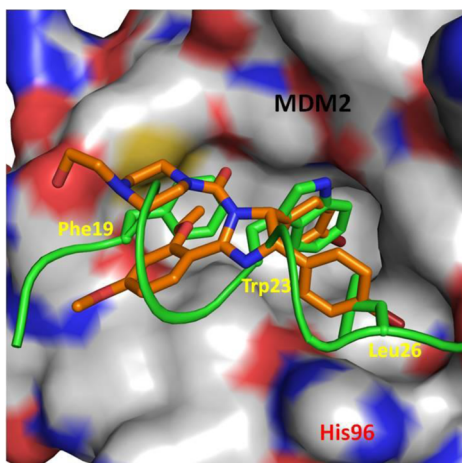


Figure 4. Cocrystal structure of 2 and MDM2. The p53 peptide is green.

Compound 1 activates wild-type p53 in cancer and normal cells but selectively kills tumor cells. It inhibits cell growth with IC<sub>50</sub> of 1–2  $\mu$ M in human cancer cell lines with wild-type p53 (SJSAs-1, HCT116, and RKO) and demonstrates approximately 10-fold selectivity over cancer cells harboring mutated p53 (MDA-MB-435 and SW480).<sup>39</sup> These observations are consistent with the hypothesis that the antitumor activity of MDM2 inhibitors should be p53-dependent. In vivo, oral administration of 1 dose-dependently activates p53 and induces expression of p53 targeted genes, including *p21* and *MDM2*. Importantly, 90% inhibition of tumor growth is achieved in the SJSAs-1 tumor xenograft model in mice upon treatment with nutlin 3 (the racemic form of 1) at 200 mg/kg orally twice a day for 20 days with no sign of toxicity in treated animals.

Further optimization of 1 to improve its binding affinity to MDM2, cellular potency, pharmacokinetics, and chemical stability ultimately yielded 3 (Figure 3),<sup>32</sup> the first MDM2 inhibitor to advance into clinical trials.<sup>31,32</sup> Four major modifications were made to 1 to yield 3: (i) dimethyl groups on the imidazoline ring were added to prevent oxidation of the imidazoline ring; (ii) an ethyl ether group replaced the isopropyl ether in 1, reducing the molecular weight slightly;

while retaining good MDM2 binding affinity; (iii) a *tert*-butyl group was used to replace the methoxyl group in 1, which is a metabolic “soft spot”; (iv) a 3-(methylsulfonyl)propyl group was introduced into the piperidine ring to enhance MDM2 binding and improve pharmacokinetic (PK) properties. Notwithstanding these substantial modifications to the 1 structure, 3 and 1 interact with MDM2 very similarly based upon superposition of their cocrystal structures (Figure 5, PBD

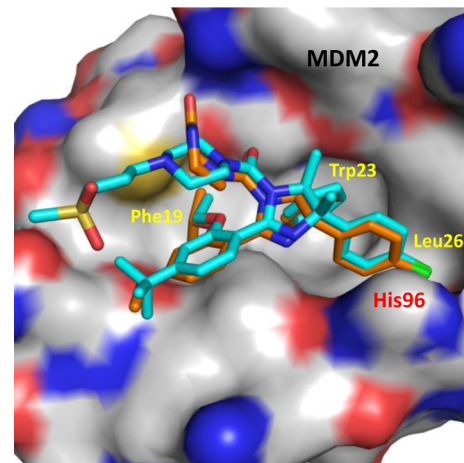


Figure 5. Superposition of cocrystal structures of MDM2 to 3 (cyan) and 1 (orange).

codes 4IPF and 4J3E). The two 4-chlorophenyl groups occupy the Trp23 and Leu26 pockets of MDM2, and the ethoxyl group is in the Phe19 pocket. The methylsulfonyl moiety of 3 extends out of the binding pocket and is exposed to solvent.

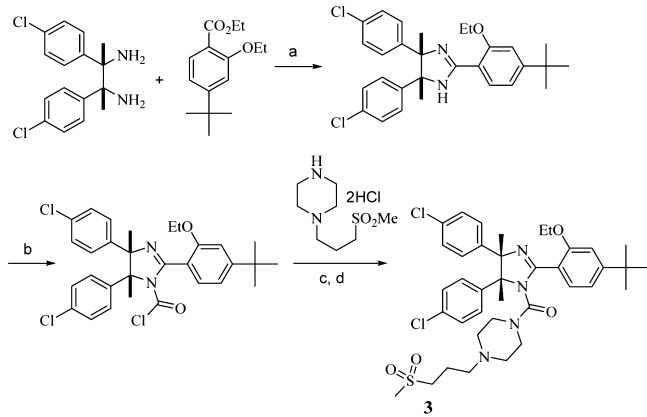
**2.1.2. Properties of the Clinical Compound 3.** Compared with 1, 3 shows enhanced MDM2 binding affinity (IC<sub>50</sub> = 18 nM). It effectively inhibits cell growth in cancer cell lines with wild-type p53 (IC<sub>50</sub> = 0.18–2.2  $\mu$ M) and demonstrates good selectivity over cancer cell lines with a p53 mutation (IC<sub>50</sub> = 5.7–20.3  $\mu$ M). 3 robustly activates wild-type p53 in vitro and in vivo, and upon oral administration at 50 mg/kg in mice, good systemic exposure is achieved with a high AUC (251.2  $\mu$ g·h/mL) and C<sub>max</sub> (15.5  $\mu$ g/mL) and slow clearance (*t*<sub>1/2</sub> = 8.8 h).

In two xenograft models of SJS1 and MHM osteosarcoma cell lines with MDM2 gene amplification and overexpression of MDM2 protein, 3 dose-dependently inhibits tumor growth and achieves partial tumor regression at 100 mg/kg daily, oral administration without signs of toxicity in mice.

**2.1.3. Results from Clinical Trials of 3.** Compound 3 has been tested in clinical trials against a wide range of cancers, including sarcoma, myelogenous leukemia, and hematologic neoplasms,<sup>31,32</sup> and results of phase I studies of 3 in chemotherapy-naïve patients with MDM2-amplified liposarcoma have recently been reported.<sup>40</sup> Upon treatment with 3, a good human PK profile was achieved and a steady state was reached on day 8. Clear activation of p53, increase in p21 protein, and apoptosis induction in tumors were observed. Treatment with 3 showed signs of antitumor activity in patients; post-treatment, 14 patients were found to have stable disease and one had a confirmed partial response. In addition, 16 out of 20 patients were treated with 3 for more than 6 months. All patients treated with 3 had at least one adverse event, and 12 serious adverse events were observed in eight patients, including neutropenia (six patients) and thrombocytopenia (three patients). It was found that exposure to 3 was correlated with hematological toxicity. On the basis of the clinical data for 3, it was concluded that the potential for late hematological toxicity, particularly thrombocytopenia, should be considered in future clinical trials of MDM2 inhibitors.<sup>40</sup>

**2.1.4. Synthesis of 3.** The synthesis of 3, based on published reports, is summarized in Scheme 1.<sup>32</sup>

**Scheme 1. Synthesis of 3<sup>a</sup>**



<sup>a</sup>Reagents and reaction conditions: (a) AlMe<sub>3</sub>, toluene, reflux; (b) phosgene, Et<sub>3</sub>N; (c) Et<sub>3</sub>N; (d) resolution by chiral chromatography.

**2.2. RG7388. 2.2.1. Discovery and Optimization.** On the basis of the structures of MI-219 (8, Figure 8)<sup>41</sup> and 3, the Hoffmann-La Roche group designed and synthesized the pyrrolidine-containing compound 4<sup>33</sup> as an MDM2 inhibitor. The two phenyl groups in 4 adopt a trans configuration, in contrast to 3 and 8 in which the two substituted phenyl groups are in a cis configuration. Compound 4 binds to MDM2 with a good affinity ( $IC_{50} = 196 \text{ nM}$ ) but is weaker than 3.

The cocrystal structure of MDM2/4 (Figure 7, PDB code 4JRG) shows that the 4-chlorophenyl group and neopentyl

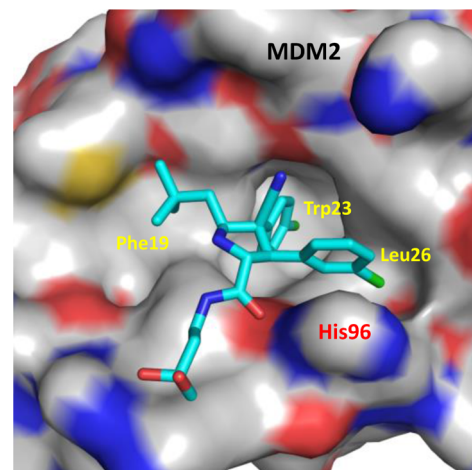
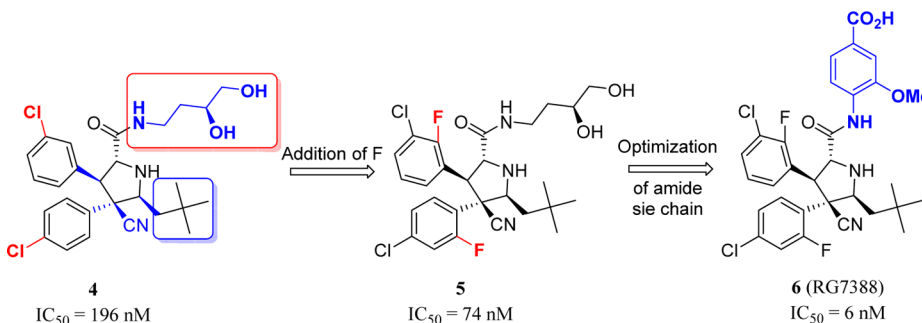


**Figure 7.** Cocrystal structure of MDM2 and 4.

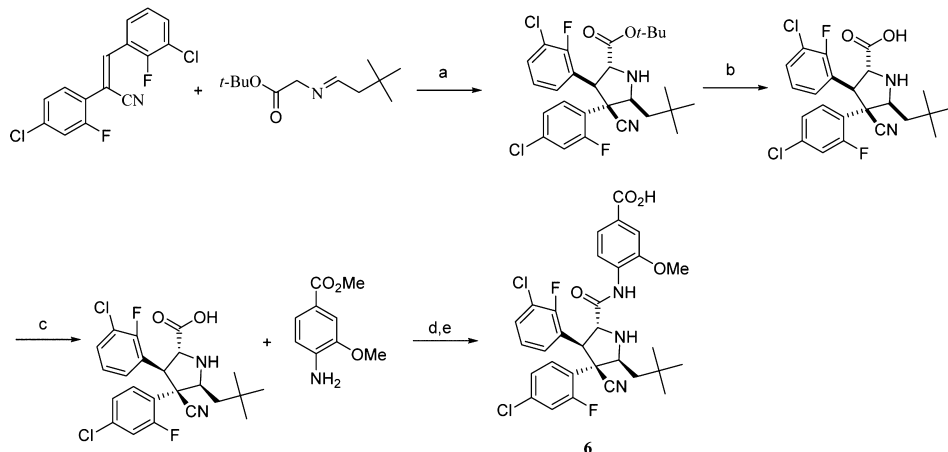
group of 4 occupy the Trp23 and Phe19 pockets, respectively, while the 2-chlorophenyl group occupies the Leu26 pocket and partakes in  $\pi-\pi$  interaction with the His96 residue. Additionally, the carbonyl group of 4 forms a hydrogen bond with NH of His96.

Pharmacokinetic studies showed that 4 has a high clearance rate and poor oral bioavailability, issues that were addressed in further modification efforts. Subsequent structure–activity relationship (SAR) analyses show that addition of fluorine atoms to the two phenyl rings of 5<sup>33</sup> enhances the MDM2 binding affinity. The dihydroxybutyl side chain of 5 was replaced with a variety of groups with the goal of improving the MDM2 binding affinity, cellular potency, microsomal stability, and PK properties. This led to the identification of *m*-methoxybenzoic acid group as an optimal group at this site, which ultimately resulted in the discovery of 6 (also known as RO5503781, Figure 6) for clinical development.<sup>33</sup>

**2.2.2. Properties of 6.** Compound 6 binds to MDM2 with  $IC_{50} = 6 \text{ nM}$ . It displays potent cell growth inhibitory activity in



**Figure 6.** MDM2 binding of pyrrolidine-containing MDM2 inhibitors.

Scheme 2. Synthesis of **6**<sup>a</sup>

<sup>a</sup>Reagents and reaction conditions: (a) AgF, Et<sub>3</sub>N, CH<sub>2</sub>Cl<sub>2</sub>, rt, 18 h; (b) CF<sub>3</sub>CO<sub>2</sub>H, CH<sub>2</sub>Cl<sub>2</sub>, rt, 18 h; (c) Resolution by chiral chromatography; (d) Ph<sub>2</sub>POCl, (i-Pr)<sub>2</sub>NEt, CH<sub>2</sub>Cl<sub>2</sub>, rt; (e) aq NaOH, THF, methanol, 40 °C.

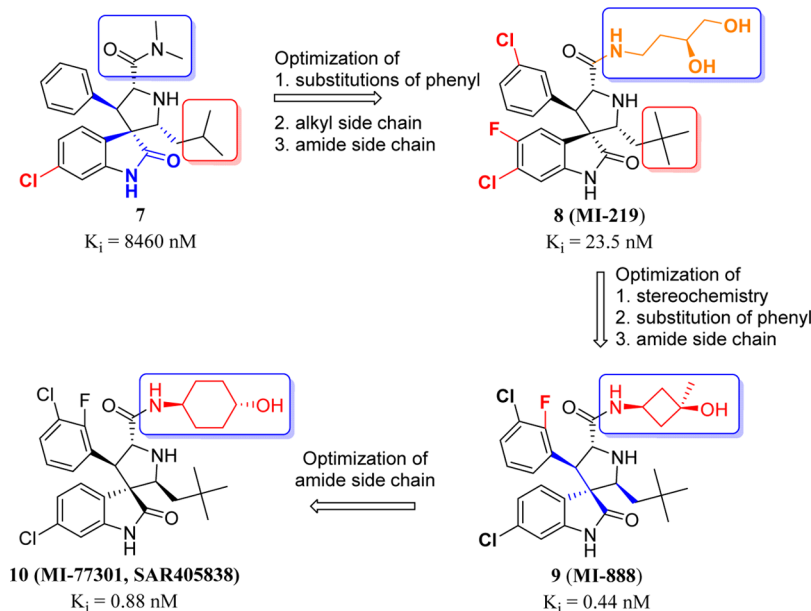


Figure 8. Structures and MDM2 binding of spiro-oxindole-containing compounds.

cancer cell lines containing wild-type p53 (average IC<sub>50</sub> = 30 nM) and displays >100-fold selectivity over cancer cell lines containing mutated p53. Furthermore, it has good microsomal stability and good PK properties. In mice, it has high oral bioavailability (80%), moderate clearance ( $t_{1/2} = 1.6$  h), and good systemic exposure and metabolic stability and is more potent than **3** and **1** in induction of p53 activation in vivo. With oral daily administration, it achieves tumor regression in the SJSA-1 osteosarcoma xenograft model in mice at 25 mg/kg. It is currently in three phase I clinical trials for treatment of patients with solid tumors, acute myelogenous leukemia, or advanced malignancies as a single agent and in combination with chemotherapeutics.<sup>42</sup>

**2.2.3. Results from Clinical Trials of **6**.** The initial phase I clinical data for **6** have recently been reported.<sup>34</sup> The maximum tolerated dose for **6** is 500 mg in a daily dosing (q.d.), 5 day schedule, 500 mg in a twice-daily (b.i.d.), 3-day schedule and 1600 mg in a b.i.d., weekly schedule. Activation of p53, as measured by MIC-1 concentration in plasma, was observed

either with daily dosing for 5 days or with b.i.d. dosing for 3 days, but it is stronger with daily, 5-day dosing. Interestingly, no clear p53 activation was observed with weekly b.i.d. dosing. Thrombocytopenia, neutropenia, febrile neutropenia, and diarrhea were the dose-limiting toxicities. FLT PET demonstrated that **6** causes decreased proliferation in tumors. The recommended phase II dose is 500 mg with daily, 5-day scheduling.

**2.2.4. Synthesis of **6**.** The published synthesis of **6** is summarized in Scheme 2.<sup>33</sup>

**2.3. MI-77301 (10, SAR405838).** **2.3.1. Discovery and Optimization.** The small molecule MDM2 inhibitor **10** (Figure 8), discovered at the University of Michigan, was advanced into phase I clinical trials by Sanofi in 2012.<sup>35,36</sup>

Compound **10** was obtained through extensive optimization of a class of spirooxindoles, such as **7**,<sup>43</sup> first reported in 2005 from our laboratory. Compound **7** was designed using a structure-based approach to mimic three key p53 binding residues (Phe19, Trp23, and Leu26) but has weak MDM2

binding affinity ( $K_i = 8.46 \mu\text{M}$ ).<sup>43</sup> Subsequent modifications of the two phenyl rings and the aliphatic and the amide side chain were carried out to improve its MDM2 binding affinity, cellular potency, and *in vivo* PK properties. Addition of a 3-chloro substituent atom on the phenyl ring and replacement of the isopropyl group with neopentyl improves the MDM2 protein binding affinity, as does replacement of the dimethylamide with a monosubstituted amine. The addition of a fluorine atom next to the chlorine on the oxindole ring generally improves the PK profile of spiro-oxindole-containing MDM2 inhibitors. Following these modifications, a potent compound, **8**<sup>41</sup> (Figure 8) was obtained. This compound binds to MDM2 with  $K_i = 23.5 \text{ nM}$  and activates wild-type p53 in cancer cells. **8** shows fairly potent cell growth inhibitory activity ( $\text{IC}_{50} \approx 1 \mu\text{M}$ ) in cancer cell lines with wild-type p53, and it is more than 10-fold less potent in cancer cells harboring mutated or deleted p53.<sup>41,44</sup> It has good oral bioavailability in rats and mice. Upon oral administration, it induces robust p53 activation in SJSAs-1 xenograft tumor tissues in mice.<sup>45</sup> Oral administration of **8** at a dose of 300 mg/kg twice daily completely inhibits tumor growth inhibition but fails to achieve tumor regression in the SJSAs-1 xenograft tumor model.<sup>41</sup>

Further optimization of **8** led to **9**<sup>44</sup> (MI-888), in which the spiro-oxindole scaffold has a different stereochemistry. The trans conformation of two substituted phenyl rings in **9** was found to be critical for improved MDM2 binding affinity. In addition, removal of the fluorine atom from the oxindole ring is beneficial to MDM2 binding affinity and addition of a single fluoro substituent on the phenyl ring improves the PK profile. Finally, the soluble tail, the *cis*-3-hydroxy-3-methyl-cyclobutylamino group, also contributes to the improved MDM2 binding affinity and a good *in vivo* PK profile. **9** has an excellent MDM2 binding affinity ( $K_i = 0.44 \text{ nM}$ ) and shows potent cell growth inhibition potency in SJSAs-1 and RS4;11 cell lines ( $\text{IC}_{50}$  of 80 and 60 nM, respectively).<sup>44</sup> It displays >100-fold selectivity for cancer cell lines with wild-type TP53 over those with mutated or deleted TP53. It is stable in mouse, rat, and human microsomes and has high systemic exposure in a mouse PK study. Oral daily administration of **9** at 100 mg/kg achieves complete and durable tumor regression in both the SJSAs-1 osteosarcoma and acute leukemia RS4;11 xenograft models in mice without signs of toxicity.

Replacement of the *cis*-3-hydroxy-3-methylcyclobutylamino group of **9** with a *trans*-4-hydroxycyclohexylamino group led to clinical compound **10**.<sup>35,36,46</sup>

### 2.3.2. Properties of Clinical Lead Compound **10**.

Compound **10** binds to MDM2 with a  $K_i$  value of 0.88 nM.<sup>36</sup> A cocrystal structure of the MDM2/**10** complex (Figure 9) was determined and provided a structural basis for its high binding affinity to MDM2. **10** mimics the three key p53 binding residues (Phe19, Trp23, and Leu26) in hydrophobic contacts and hydrogen bonding in its interaction with MDM2 but captures additional interactions. The Cl atom in the oxindole group of **10** has extensive hydrophobic contacts with MDM2. There is  $\pi-\pi$  stacking between the His96 of MDM2 and the 2-fluoro-3-chlorophenyl in **10**, and a hydrogen bond between the imidazole side chain of His96 and the carbonyl group in **10**. Interestingly, the N-terminus of MDM2 (residues 10–18) refolds and enjoys extensive interactions with **10** through Val14 and Thr16, which contributes 25-fold to the binding affinity. In contrast, the N-terminus of MDM2 (residues 1–18) has no significant contribution to the binding of p53 peptides and **1**.

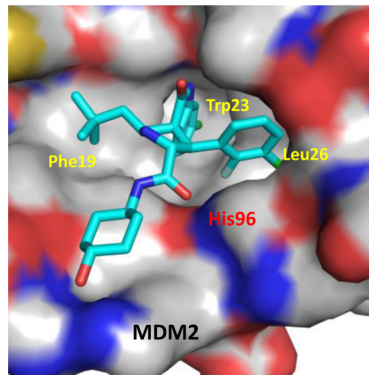


Figure 9. X-ray cocrystal structure of MDM2/**10**.

Compound **10** inhibits cell growth with  $\text{IC}_{50}$  values of 100–200 nM in SJSAs-1, RS4;11, LNCaP, and HCT116 cancer cell lines containing wild-type p53 and demonstrates >100-fold selectivity over cancer cell lines with mutated or deleted p53.<sup>36</sup> Compound **10** effectively activates wild-type p53 in cancer cell lines at concentrations as low as 30 nM *in vitro* and in xenograft tumor tissue of leukemia and solid tumors, leading to p53-dependent cell cycle arrest and/or apoptosis in tumor cells. With daily oral administration at 100 mg/kg, it achieves complete and durable tumor regression in mouse xenograft models of SJSAs-1 osteosarcoma and RS4;11 acute leukemia, partial (80%) regression in the LNCaP prostate cancer xenograft model, and complete tumor growth inhibition in the HCT116 colon cancer xenograft model. A single oral dose of compound **10** at 200 mg/kg induces strong apoptosis in the SJSAs-1 tumor tissue with the effect lasting for >3 days and complete tumor regression in 100% of animals. Mechanistically, robust transcriptional up-regulation of PUMA induced by **10** is associated with robust apoptosis in cancer cell lines *in vitro*, tumor tissue *in vivo*, and complete tumor regression in xenograft models in mice. These preclinical data suggest the strong therapeutic potential of compound **10** for the treatment of different types of human cancer.

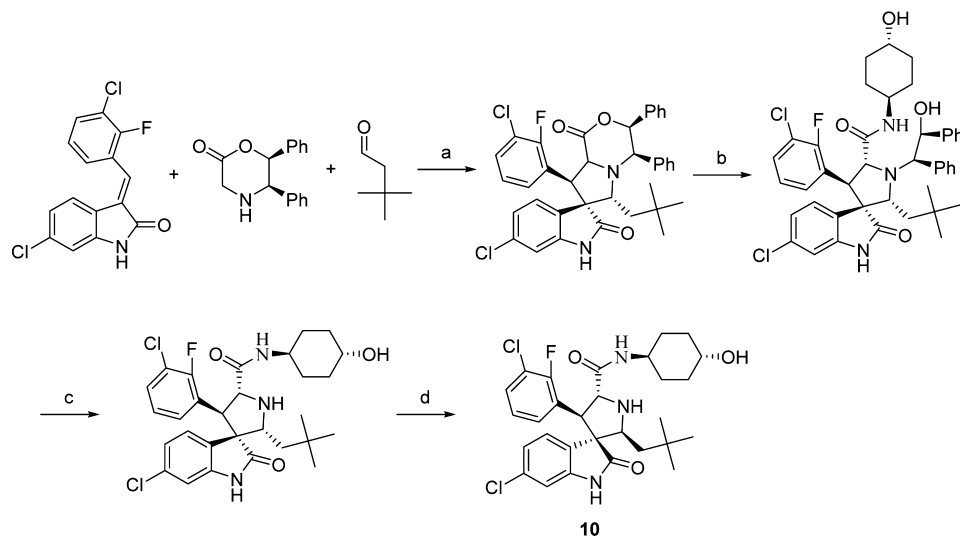
In 2012, Sanofi initiated a phase I clinical trial of compound **10** to assess its safety, tolerability, pharmacokinetics, and biological activity in patients with advanced cancer.<sup>35</sup> A second phase I trial was initiated in 2013 to evaluate **10** in combination with pimasertib, an allosteric inhibitor of MEK1/2 in patients with solid tumors.<sup>35</sup> The phase I clinical trial results for **10** have not been published.

**2.3.3. Synthesis of **10**.** The synthesis of **10** is shown in Scheme 3.<sup>44,47</sup>

### 2.4. AMG 232. 2.4.1. Discovery and Optimization.

Compound **14** (Figure 10), discovered and developed by Amgen, entered phase I clinical trials for the treatment of human cancer in 2012.<sup>37,38</sup> This compound was obtained through structure-based design and extensive optimization of a new class of MDM2 inhibitors containing piperidin-2-one.<sup>38,48</sup>

The piperidinone-containing compound **11**<sup>48</sup> (Figure 10) was designed as an MDM2 inhibitor based upon a structural analysis of known MDM2 inhibitors, such as **1**, **8**, and a previously reported MDM2 inhibitor by Amgen, to mimic three key binding residues in p53. Compound **11** binds to MDM2 with  $\text{IC}_{50} = 34 \text{ nM}$  and served as an excellent lead compound for further optimization. Upon the basis of the NMR and cocrystal structures of **11** or its analogues complexed with MDM2 (Figure 11, PDB codes 4HMB and 2LZG),<sup>49</sup> further

Scheme 3. Synthesis of **10**<sup>a</sup>

<sup>a</sup>Reagents and reaction conditions: (a) toluene, molecular sieves 4 Å, reflux overnight; (b) *trans*-4-aminohexanol, THF, rt, 2 days; (c) CAN, acetonitrile-H<sub>2</sub>O-acetone, ice bath, 5 min; (d) methanol-H<sub>2</sub>O, rt, 1–4 days.

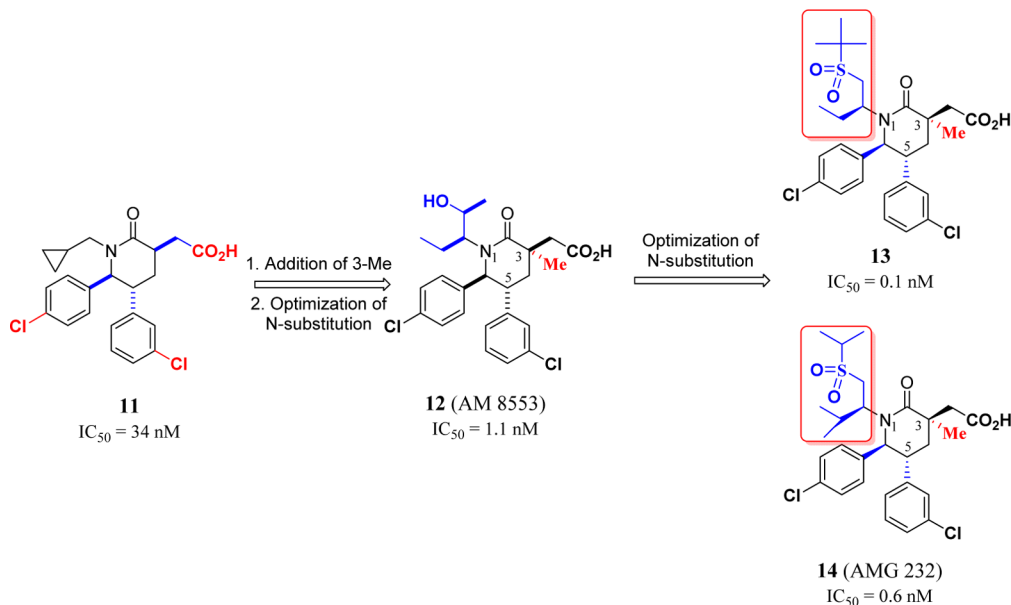


Figure 10. Structures of piperidinone-containing compounds.

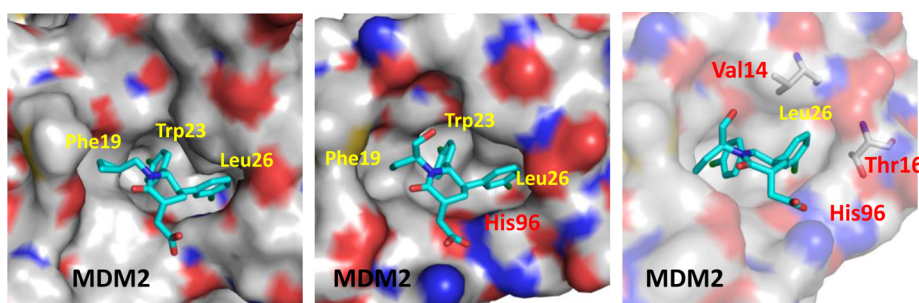


Figure 11. NMR structure of MDM2/11 (left) and X-ray crystal structures of MDM2/11 analogue (middle and right).

optimization of two sites of **11** yielded **12** (AM 8553),<sup>48</sup> which has an IC<sub>50</sub> value of 1.1 nM to MDM2 ( $K_d = 0.4$  nM to MDM2). Compound **12** effectively activates wild-type p53 in vitro and in vivo and dose-dependently inhibits tumor growth

in the SJS-A-1 xenograft model in mice. At 150 and 200 mg/kg daily oral dosing for 2 weeks, it achieves partial tumor regression (27%) after 2 weeks of treatment. It was further optimized for potency, pharmacokinetic properties, and in vivo

efficacy. This yielded a series of potent and orally active MDM2 inhibitors including **13**<sup>38</sup> and **14**, whereas the latter was selected for clinical development.

Several high-resolution cocrystal structures of MDM2 complexed with members of this class of MDM2 inhibitors have been determined<sup>38,48,49</sup> and provide structural insights into their high affinity binding. In the MDM2/**13** cocrystal structure (Figure 12, PDB code 4OAS), the 3-chlorophenyl and

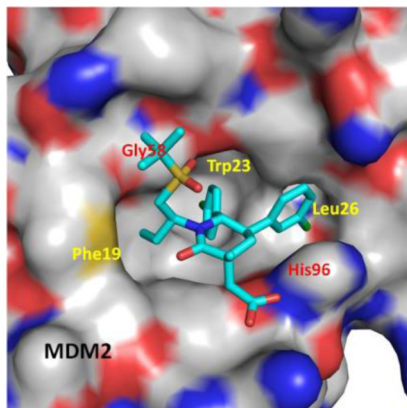


Figure 12. X-ray cocrystal structure of MDM2/13 (cyan).

4-chlorophenyl groups project into the Leu26 and Trp23 pockets, respectively.<sup>38</sup> The Phe19 pocket is occupied by the ethyl group. The sulfonyl *tert*-butyl group resides in the small pocket around G58, and the carboxylic acid forms a salt bridge with the His96 residue of MDM2. The cocrystal structure for MDM2/**14** has not been reported, but Amgen scientists predict that **14** has a similar binding model as **13**.<sup>38</sup> Furthermore, binding between inhibitors in this class (e.g., **11**) and MDM2

induces reorganization of the extreme N-terminus of the MDM2 protein and promotes additional hydrophobic contacts between the *m*-chlorophenyl moiety in the inhibitors and the Val14 and Thr16 residues in MDM2 (Figure 11, right).<sup>49</sup> Hence, **14** not only mimics the three key p53 residues but captures additional interactions not observed between p53 and the refolded MDM2 to achieve a very high binding affinity with MDM2.

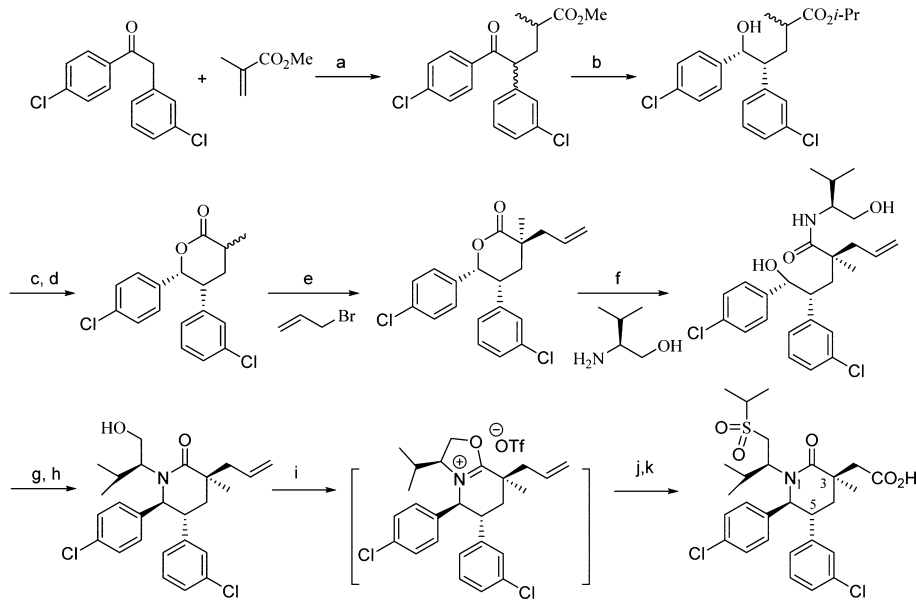
#### 2.4.2. Properties of Clinical Lead Compound **14**.

Compound **14** binds to MDM2 with  $IC_{50} = 0.6$  nM in a competitive binding assay and has a  $K_d$  value of 0.045 nM with MDM2, determined by surface plasmon resonance (SPR).<sup>38</sup> It potently inhibits cell proliferation with  $IC_{50}$  values of 9.1 and 10 nM in an BrdU proliferation assay in the SJSA-1 and HCT-116 cell lines, respectively, and demonstrates over >1000-fold selectivity over the HCT-116 p53 knockout ( $p53^{-/-}$ ) cell line. In efficacy studies using human tumor xenograft models in mice, it effectively inhibits tumor growth in the SJSA-1 osteosarcoma model with an  $ED_{50}$  of 9.1 mg/kg with daily oral administration and demonstrates complete tumor regression in 10 of 12 animals treated with 60 mg/kg daily. It also effectively and dose-dependently inhibits tumor growth in the HCT-116 xenograft model with twice daily dosing with an  $ED_{50}$  of 16 mg/kg and achieves tumor stasis (100% tumor growth inhibition) without tumor regression. In preclinical safety evaluations, no significant liability was found for **14** to preclude it from clinical development; it was projected to have a low clearance rate and consequently a long half-life in humans.

2.4.3. Synthesis of **14**. The synthesis of **14** is shown in Scheme 4.<sup>38,50</sup>

2.5. Other MDM2 Inhibitors in Clinical Trials. The MDM2 inhibitor MK-8242,<sup>41</sup> also known as SCH 900242,<sup>51</sup> developed by Merck has been tested since 2011 as a single

Scheme 4. Synthesis of **14**<sup>a</sup>



**14**

<sup>a</sup>Reagents and reaction conditions: (a) 10% *t*-BuOK, THF, rt, 2 d; (b) 0.2% RuCl<sub>2</sub>[(*S*-xylBINAP)(*S*-DAIPEN)], 40% *t*-BuOK, *i*-PrOH, H<sub>2</sub> (50 PSI), rt, 65 h; (c) LiOH, THF/MeOH/H<sub>2</sub>O; (d) PPTS, toluene, reflux; (e) LiHMDS, allyl bromide, THF; (f) neat, 100 °C, overnight; (g) Tf<sub>2</sub>O, 2,6-lutidine, CH<sub>2</sub>Cl<sub>2</sub>, -78 to 0 °C; (h) aq NaHCO<sub>3</sub>; (i) Tf<sub>2</sub>O, 2,6-lutidine. (j) Method A: *i*-PrSnNa, DMF. Method B: *i*-PrSO<sub>2</sub>Na, acetonitrile. Method C: *i*-PrSH, base, DMF. (k) RuCl<sub>3</sub>, NaIO<sub>4</sub>, acetonitrile/CCl<sub>4</sub>/H<sub>2</sub>O.

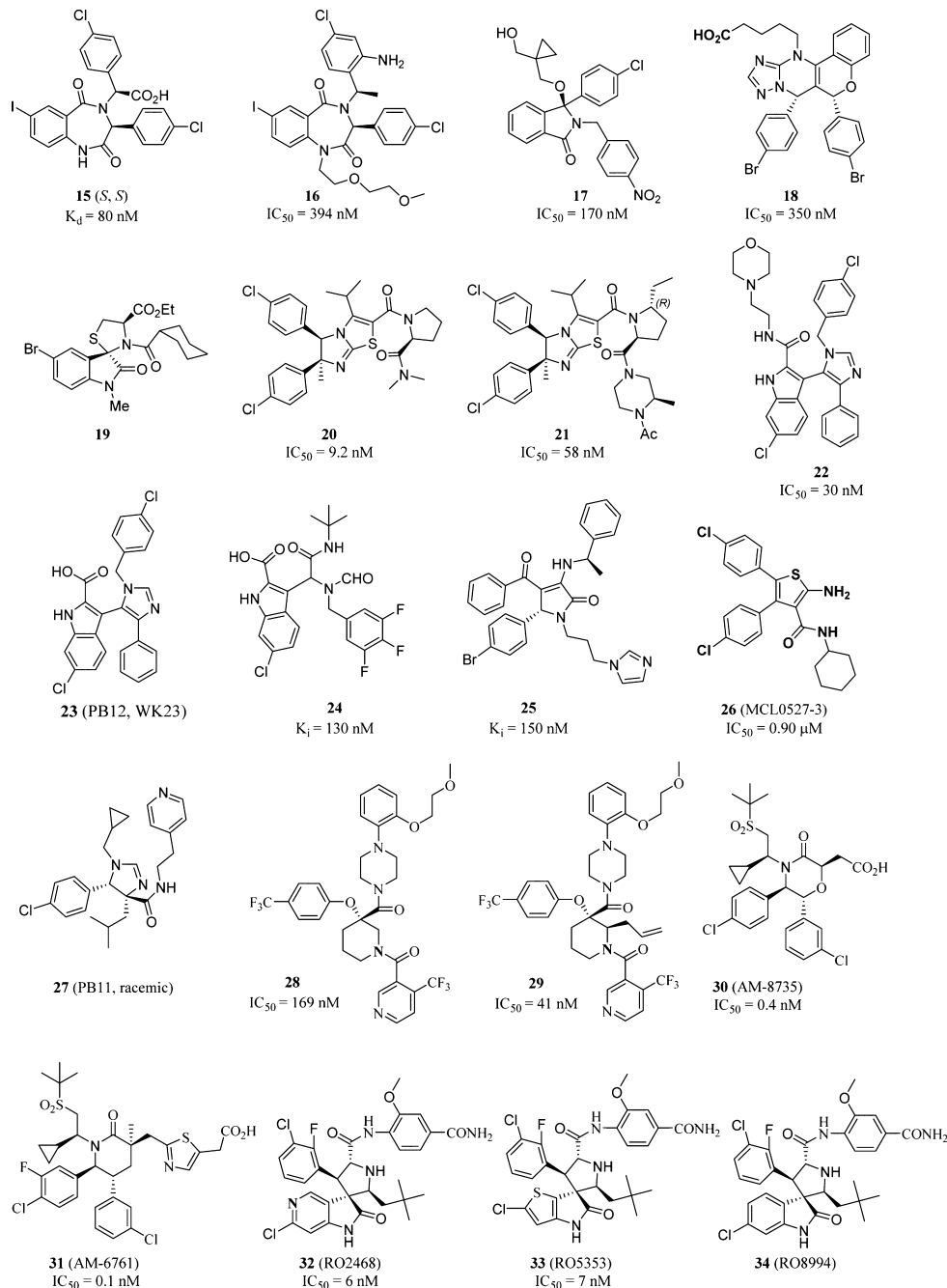


**Figure 13.** Examples of reported MDM2 inhibitors in the literature.

agent or in combination with cytarabine in patients with advanced solid tumors or leukemia. The MDM2 inhibitors, CGM097 (35)<sup>39</sup> developed by Novartis International AG and DS-3032b (36)<sup>40</sup> developed by Daiichi Sankyo Inc., have also entered phase I clinical trials in 2013. Compound 35 is to be tested in selected patients who have advanced solid tumors with p53 wild status. Compound 36 will be tested in patients who have advanced solid tumors or lymphomas. The chemical structures and preclinical data for these three clinical-stage MDM2 inhibitors have not been disclosed.

### 3. OTHER MDM2 INHIBITORS REPORTED BY INDUSTRIAL AND ACADEMIC GROUPS

In addition to the seven compounds that have been advanced into clinical development, there are several additional classes of

MDM2 inhibitors that have been reported by industrial and academic groups. Johnson & Johnson reported a class of benzodiazepine-containing compounds as MDM2 inhibitors.<sup>52</sup> One of the better compounds they reported was 15 (Figure 13 and Table 2), which had MDM2 binding affinity ( $K_d = 80 \text{ nM}$ ), while its corresponding enantiomer was 50 times less potent.<sup>53,54</sup> Compound 15 has low cell permeability, rapid in vivo clearance, and low bioavailability.<sup>53</sup> Subsequent modifications led to 16, in which soluble tails were added and the carboxylic acid moiety was replaced by a substituted benzyl group.<sup>55</sup> Compound 16 shows MDM2 binding ( $IC_{50} = 394 \text{ nM}$ ) and BrdU incorporation ( $IC_{50} = 1.1 \mu\text{M}$ ) in the MCF-7 cell line.

Researchers at the University of Newcastle reported isoindolinone-containing compounds as MDM2 inhibi-

Table 2. Summary of Other MDM2 Inhibitors

entry	compd	MDM2 binding IC <sub>50</sub>	cell line; assay; IC <sub>50</sub>	PDB code	in vivo data	ref
1	<b>15</b>	80 nM <sup>a</sup>	MCF7; BrdU; 38 $\mu$ M	1T4E		53, 54
2	<b>16</b>	394 nM	MCF7; BrdU; 1.1 $\mu$ M			55
3	<b>17</b>	170 nM	SJSA-1; SRB; 5.2 $\mu$ M			56
4	<b>18</b>	350 nM	SJSA-1; p21; 12 $\mu$ M		PK data	57
5	<b>19</b>	>5 $\mu$ M	MCF-7; MTT; 40 nM			58
6	<b>20</b>	9.2 nM		3VZV		59
7	<b>21</b>	58 nM	MV4;11; luminescent; 220 nM	3W69	PK and efficacy in SCID mice	59
8	<b>22</b>	30 nM		4DIJ		60
9	<b>23</b>	916 nM <sup>b</sup>		3LBK		61
10	<b>24</b>	130 nM <sup>b</sup>				62
11	<b>25</b>	150 nM <sup>b</sup>	AS49; MTT; 1.97 $\mu$ M		efficacy in nude mice	63
12	<b>26</b>	0.90 $\mu$ M	SJSA-1; SRB; 102.3 $\mu$ M			64
13	<b>27</b>	0.8 $\mu$ M <sup>a</sup>				61
14	<b>28</b>	169 nM	SJSA-1; 4.7 $\mu$ M			65, 66
15	<b>29</b>	41 nM	SJSA-1; 1 $\mu$ M			65, 66
16	<b>30</b>	0.4 nM	SJSA-1; EdU; 25 nM	4OBA	PK and efficacy in nude mice	67
17	<b>31</b>	0.1 nM	SJSA-1; EdU; 16 nM	4ODE	PK and efficacy in nude mice	68
18	<b>32</b>	6 nM	av of three; <sup>c</sup> MTT; 15 nM		PK and efficacy in nude mice	69
19	<b>33</b>	7 nM	av of three; <sup>c</sup> MTT; 7 nM	4LWV	PK and efficacy in nude mice	69

<sup>a</sup>Binding affinity was measured as K<sub>d</sub>; <sup>b</sup>Binding affinity was measured as K<sub>i</sub>; <sup>c</sup>Average of three cell lines SJSA-1, HCT116, and RKO

tors.<sup>56,70,71</sup> Subsequent optimization efforts guided by NMR analysis led to the identification of compound **17** (Figure 8),<sup>56</sup> which has binding affinity to MDM2 (IC<sub>50</sub> = 0.17  $\mu$ M) in an ELISA assay and cell growth inhibition (GI<sub>50</sub> = 5.2  $\mu$ M) in the SJSA-1 cell line.

In addition to **14**, scientists from Amgen reported a class of chromenotriazolopyrimidine<sup>72</sup> compounds as MDM2 inhibitors. Extensive modifications of these compounds led to **18**,<sup>57</sup> which binds to MDM2 with IC<sub>50</sub> = 350 nM and shows moderate cellular activity and microsomal stability, high oral bioavailability (54%), and slow clearance in rodents.

In 2010, a class of spiro(oxindole-3,3'-thiazolidine)-containing compounds was first reported as possible MDM2 inhibitors.<sup>73</sup> Chemical modifications led to **19**,<sup>58</sup> which has cellular growth inhibition activity >20 times that of nutlin-3 in a selected subset of cancer cell lines.

Researchers from Daiichi Sankyo reported a class of 5,6-dihydroimidazo[2,1-*b*][1,3]thiazol-containing compounds (**20**, **21**) as potent MDM2 inhibitors.<sup>59</sup> **20** has high MDM2 binding affinity (IC<sub>50</sub> = 9.2 nM) but poor metabolic stability, resulting in weak *in vivo* antitumor efficacy in an MV4-11 xenograft model. After extensive modifications, **21** was obtained and shows high MDM2 binding potency (IC<sub>50</sub> = 58 nM), moderate solubility (25  $\mu$ g/mL) in pH 6.8 phosphate buffer, good hepatic microsomal stability, and high systemic exposure in mice. It also showed ~50-fold selectivity in TP53 wild type over TP53-mutated cell lines (GI<sub>50</sub> = 0.22  $\mu$ M in MV4;11 vs GI<sub>50</sub> = 10  $\mu$ M in DLD-1). Upon oral administration of **21** at a daily dose of 200 mg/kg, 76% TGI was achieved at the end of treatment in mouse MV4;11 tumor xenograft model with no sign of acute toxicity.

A class of compounds featuring a 3-(1*H*-imidazol-5-yl)-1*H*-indole-2-carboxylic acid structure was reported independently by two groups. Scientists from Novartis reported **22**, which has an MDM2 binding affinity of IC<sub>50</sub> = 30 nM.<sup>60</sup> In addition, **23** was synthesized by Dömling's group at the University of Pittsburgh by means of a three-component reaction<sup>61</sup> and was found to have MDM2 binding affinity (K<sub>i</sub> = 916 nM)<sup>74</sup> in a fluorescent polarization assay. Another class of 2-indolecarbox-

ylic acid containing MDM2 inhibitors also has three hydrophobic groups converging on a sp<sup>3</sup> carbon and **24**; the best of these compounds binds to MDM2 with K<sub>i</sub> = 130 nM.<sup>62</sup>

In 2012, 1*H*-pyrrolone-containing compounds, such as **25**, were reported as MDM2 inhibitors. **25** has MDM2 binding (K<sub>i</sub> = 0.15  $\mu$ M) and cell growth inhibition (IC<sub>50</sub> ≈ 1.97–28.11  $\mu$ M) in Saoc-2, U-2OS, A549, and NCI-H1299 cell lines.<sup>63</sup> Using pharmacophore-based virtual screening, Wang and co-workers identified thiophene-containing compounds as MDM2 inhibitors.<sup>64</sup> One of the most potent of these compounds, MCL0527-3 (**26**), shows MDM2 binding affinity (IC<sub>50</sub> = 0.90  $\mu$ M) and cell growth inhibition (IC<sub>50</sub> of 2.41, 0.59, and 102.3  $\mu$ M in A549, HCT116, and SJSA-1 cell lines, respectively). A dihydroimidazole-containing compound PB11 (**27**), synthesized from a multiple component reaction followed by amidation, has MDM2 binding affinity (K<sub>d</sub> = 0.8  $\mu$ M).<sup>61</sup>

Merck scientists recently reported a class of piperidine-containing compounds (**28**, **29**) with MDM2 binding (IC<sub>50</sub> of 169 and 41 nM, respectively).<sup>65,66,75</sup> Detailed SAR studies and computational calculations suggested that substituents on the 2-position of the piperidine ring, for example the allyl moiety of **28**, can stabilize the binding conformation of the piperidine ring and are compatible with both polar and nonpolar functional groups. However, both compounds **28** and **29** inhibit CYP 3A4 (IC<sub>50</sub> < 5  $\mu$ M), a liability that may need to be addressed for further development for this class of compounds.

A class of morpholinone-containing MDM2 inhibitors, such as **30**, was recently reported by Amgen scientists.<sup>67</sup> Compound **30** has MDM2 binding (IC<sub>50</sub> = 0.4 ± 0.1 nM) and BrdU incorporation (IC<sub>50</sub> = 25 ± 9 nM) in the SJSA-1 cell line. With oral administration of **30** at 100 mg/kg daily, partial tumor regression was achieved at the end of treatment in an SJSA-1 female athymic nude mice xenograft. Most interestingly, **30** has slower clearance in rats and higher hepatocyte stability than the corresponding piperidinone-containing analogue. Metabolite profiling showed that metabolic oxidation and glucuronidation of **30** are significantly slower than those of its corresponding piperidinone-containing analogue. These data indicate that morpholinone-containing MDM2 inhibitors such as **30** do have

advantages in their DMPK profile relative to piperidinone-containing MDM2 inhibitors such as **14**. Additional modification of **14** focused on replacement of its carboxylic acid moiety with corresponding isosteres.<sup>68</sup> It was interesting to find that heterocycles such as a thiazole group are a good replacement for the carboxylic acid group and forms hydrogen bonds with the imidazole NH of His96 through the nitrogen atom. This modification led to identification of **31** (AM 6761), which has good MDM2 binding ( $IC_{50} = 0.1$  nM), good cellular potency (SJS-1  $IC_{50} = 16$  nM), and favorable pharmacokinetic properties. Upon oral administration of **31** at a daily dose of 50 mg/kg, 5.6% tumor regression was achieved in SJS-1 female athymic nude mice xenografts after 12 days of treatment. The metabolite profiles of **31** in mouse, rat, dog, monkey, and human hepatocytes suggest that **31** is primarily cleared through oxidative pathways and thus is distinct from the main metabolism of **14** which is through glucuronidation.

Very recently, Zhang and coauthors reported **32** (RO2468) and **33** (RO5353) as potent MDM2 inhibitors with useful in vivo antitumor activity.<sup>69</sup> The medicinal chemistry optimization was based on **34** (RO8994) and the clinical drug **6** and featured incorporation of a pyridine or thiophene ring as a replacement of one of the phenyl rings of **34**. Compounds **32** and **33** have MDM2 binding in the low nanomolar region, with average cellular  $IC_{50}$  values in three cancer cell lines of 15 and 7 nM, and good oral pharmacokinetic profiles comparable to that of **6**. Upon oral administration of **32** at 10 mg/kg daily dose, complete tumor regression is achieved in SJS-1 nude mice xenograft at the end of a 14-day treatment. In the same mouse tumor model, oral administration of **33** at a daily dose of 10 mg/kg also achieves significant tumor regression.

#### 4. CONCLUDING REMARKS AND OUTLOOK FOR SMALL-MOLECULE MDM2 INHIBITORS AS A NEW CLASS OF DRUGS FOR CANCER TREATMENT

Intense research efforts in the past decade have led to the discovery of a number of classes of highly potent and selective MDM2 inhibitors, and seven such compounds are now in clinical trials. Several of these clinically tested MDM2 inhibitors bind to MDM2 with a very high affinity ( $K_d$  or  $K_i$  of <1 nM) and demonstrate significant selectivity over MDMX, a homologue of MDM2, and other proteins tested. Cocrystal structures of a large number of high-affinity inhibitors in complex with MDM2 show that these MDM2 inhibitors not only mimic the three key p53 binding residues (Phe19, Trp23, and Leu26) but also capture additional interactions not observed between p53 and MDM2. In particular, both **10** and **14** have  $\pi-\pi$  stacking with His96 and induce refolding of the extreme N-terminus of MDM2, gaining additional hydrophobic interactions, with residues Thr12 and Val14.<sup>36,49</sup> Furthermore, **14** also forms a surface electrostatic interaction with the G58 “shelf” region in MDM2. As a result, these small-molecule MDM2 inhibitors can achieve binding affinities to MDM2 that are >1000 times better than the affinities of p53 peptides. Pharmacokinetic properties, including oral bioavailability, have also been extensively optimized for these clinical-stage MDM2 inhibitors. The successful discovery of these highly potent and selective MDM2 inhibitors with optimized pharmacokinetic properties is a success of modern medicinal chemistry in targeting protein–protein interactions.

When the interaction of MDM2 with p53 is blocked, these potent MDM2 inhibitors inhibit MDM2-mediated p53 ubiquitination and degradation, leading to accumulation and

activation of p53 protein in cells with wild-type p53. Activation of p53 results in transcription of p53-targeted genes, including p21,<sup>76</sup> a cell cycle regulator, and PUMA,<sup>77</sup> a proapoptotic protein, leading to cell cycle arrest and/or apoptosis in tumor cells. Since MDM2 is also a p53-targeted gene, MDM2 inhibitors also induce up-regulation of MDM2 mRNA and protein.<sup>20,39</sup> As expected, these potent and selective MDM2 inhibitors dose-dependently and effectively activate p53 in tumor cells with wild-type p53 but not in tumor cells harboring mutated or deleted p53. They potently inhibit cell growth in cancer cell lines with wild-type p53 and show high selectivity over cancer cell lines with mutated or deleted p53. Interestingly, while MDM2 inhibitors can inhibit cell cycle progression in all tumor cell lines with wild-type p53, they effectively induce apoptosis in only some cancer cell lines.<sup>78</sup> Analysis of p53-regulated proapoptotic genes, PUMA, Noxa, and Bax, in a number of cancer cell lines revealed that PUMA, but not Noxa and Bax, was induced by MDM2 inhibitors and the magnitude of PUMA induction correlates with the degree of apoptosis induction.<sup>36</sup>

Although earlier generations of MDM2 inhibitors such as **1** and **8** are capable of inhibiting 100% tumor growth in xenograft models of human cancer, they are unable to achieve complete tumor regression. However, recently discovered MDM2 inhibitors such as **10** and **14**, with improved binding affinities to MDM2, cellular potencies, and significantly optimized pharmacokinetic properties, can effectively induce complete tumor regression in the SJS-1 osteosarcoma xenograft model in mice. The SJS-1 osteosarcoma cell line has MDM2 gene amplification and is sensitive to MDM2 inhibitors in apoptosis induction. Although only ~7% of all human cancers have an amplified MDM2 gene,<sup>14</sup> a higher frequency of MDM2 gene amplification occurs in certain tumor types, including well-differentiated liposarcomas (>80%), soft tissue tumors (20%), osteosarcomas (16%), and esophageal carcinomas (13%).<sup>79,80</sup> The complete tumor regression achieved by these new MDM2 inhibitors in the SJS-1 xenograft model suggests their therapeutic potential as single agents for the treatment of human cancers with MDM2 gene amplification. Additionally, MDM2 inhibitors such as **6** and **10** have been shown to achieve tumor regression in leukemia xenograft models in mice.<sup>33,36</sup> In other xenograft models, such as the xenograft model of the HCT-116 colon cancer cell line, MDM2 inhibitors effectively inhibit tumor growth (tumor stasis) but fail to achieve tumor regression.<sup>36</sup> This is consistent with their ability to effectively inhibit cell cycle progression and their inability to induce apoptosis in the HCT-116 cell line. Taken together, these in vivo data suggest that MDM2 inhibitors may have a strong therapeutic potential for the treatment of a subset of human solid tumors and leukemia.

In addition to the development of MDM2 inhibitors as single agents, MDM2 inhibitors have been evaluated in combination with both traditional chemotherapeutic agents and molecularly targeted agents. These potent MDM2 inhibitors in clinical development are highly selective for MDM2, but they fail to target MDMX, which directly interacts with p53 and inhibits its function. Since a number of chemotherapeutic agents such as irinotecan and doxorubicin can effectively down-regulate MDMX, their combination with MDM2 inhibitors can be very effective for the treatment of human cancers with high expression of both MDM2 and MDMX proteins. In addition to these traditional chemotherapeutic agents, MEK inhibitors such as trametinib are very effective in induction of down-regulation

of MDMX.<sup>81</sup> Indeed, MEK inhibitors such as trametinib and pimasetib are currently being evaluated in combination with either **10** or **14** in clinical trials for the treatment of patients with acute myeloid leukemia or solid tumors.<sup>35,37</sup>

Acquired resistance of tumor cells to cancer drugs is a major clinical challenge in drug development. Because MDM2 inhibitors are only effective in targeting tumor cells with wild-type p53, they may select resistant tumor cells that acquire p53 mutation(s) that escape MDM2 control. Indeed, treatment of SJSA-1 cells with nutlin 3 in cell cultures has resulted in selection of colonies that contain p53 mutations in DNA binding domain and become highly resistant to nutlin 3.<sup>82</sup> Therefore, combinations of MDM2 inhibitors with agents that are effective against tumor cells with p53 mutations should be tested to prevent or delay acquired resistance.

Since MDM2 inhibitors also activate p53 in normal cells and normal tissues, there is a concern that activation of p53 can cause toxicity in those normal tissues sensitive to p53 activation, such as bone marrow, spleen, and small intestines. Data from phase I clinical trials of **3**<sup>40</sup> and **6**<sup>34</sup> showed that these MDM2 inhibitors cause thrombocytopenia (decrease of platelets in blood), which is a major dose-limiting toxicity. Mechanistic studies<sup>83</sup> showed that **3** promoted apoptosis of megakaryocyte (MK) progenitor cells, resulting in a reduction of their numbers and affected mature MK cells by blocking DNA synthesis during endomitosis and impairing platelet production. Therefore, determination of appropriate dose schedules that can achieve robust p53 activation and strong antitumor activity but have manageable on-target toxicity will be another critical task for the successful development of these potent MDM2 inhibitors.

## AUTHOR INFORMATION

### Corresponding Author

\*Phone: 734-615-0362. Fax: 734-647-9647. E-mail: shaomeng@umich.edu.

### Notes

The authors declare the following competing financial interest(s): Drs. Shaomeng Wang and Yujun Zhao are inventors on MI-77301, which is being developed by Ascenta and Sanofi and received royalties from the University of Michigan. Dr. Shaomeng Wang also owns stock in Ascenta and has received research funding from Ascenta and Sanofi.

### Biographies

**Yujun Zhao** is a Research Investigator in Division of Hematology/Oncology, University of Michigan. He completed a Ph.D in Organic Chemistry at Nanyang Technological University (Singapore) under the supervision of Prof. Teck-Peng Loh. He joined Prof. Shaomeng Wang's lab as a Research Fellow in 2009 where he contributed to the nomination of SAR405838 as a potent MDM2 inhibitor for human clinical trials. His research interest includes asymmetric synthesis and small-molecule modulation of protein–protein interactions.

**Angelo Aguilar** is a Research Investigator in the Department of Internal Medicine-Hematology/Oncology at the University of Michigan in Ann Arbor, MI. Prior to becoming a Research Investigator, he joined Professor Wang's group as a postdoctoral fellow in 2009. Before joining the University of Michigan, Dr. Aguilar earned his Ph.D. in Organic Chemistry from Kansas State University under the guidance of Professor Duy H. Hua. Dr. Aguilar received his B.S. in Chemistry from Regis University in Denver, CO, and then went on to work as an Analyst I at Severn-Trent Laboratories in Denver-Arvada, CO, until starting his Ph.D.

**Denzil Bernard** received training in pharmacy at the Institute of Chemical Technology, formerly the University Department of Chemical Technology Mumbai, India, and got his Bachelor's degree in Pharmaceutical Sciences from the University of Mumbai, India. He completed his Ph.D. in Pharmaceutical Sciences from the University of Maryland, focusing on computer-aided drug design, leading to the development of the conformationally sampled pharmacophore (CSP) model. His research interests are in the development and application of computational tools for drug design. He is currently a Research Specialist at the University of Michigan, and his primary focus is on the development of novel anticancer agents.

**Shaomeng Wang** is a Warner-Lambert/Parke-Davis Professor in Medicine and Professor of Medicine, Pharmacology, and Medicinal Chemistry and the Director of the Cancer Drug Discovery Program at the University of Michigan. He received his B.S. in Chemistry from Peking University, China, in 1986 and Ph.D. in Chemistry from Case Western Reserve University, OH, U.S., in 1992. He did his postdoctoral training at the National Cancer Institute, NIH, between 1992 and 1996. He was Assistant Professor and then Associate Professor between 1996 and 2001 at Georgetown University and joined the University of Michigan in 2001. He has advanced four novel small-molecule anticancer drugs into clinical development and won a number of awards for his work. He has served as the Editor-in-Chief of *Journal of Medicinal Chemistry* since 2012.

## ACKNOWLEDGMENTS

We thank the present and past members of the Wang laboratory at the University of Michigan, who have contributed to the MDM2 project, and our collaborators and partners, who have made it possible to advance MI-77301 into clinical development. In particular, we deeply appreciate the financial support from the National Cancer Institute (NCI), National Institutes of Health (NIH), the Prostate Cancer Foundation, the Leukemia and Lymphoma Society, Ascenta Therapeutics, and Sanofi for our MDM2 research project.

## ABBREVIATIONS USED

CAN, ceric ammonium nitrate; MTT, 3-(4,5-dimethylthiazol-2-yl)-2,5-diphenyltetrazolium bromide mediated cell growth inhibition assay; PK, pharmacokinetics; PPTS, pyridinium *p*-toluenesulfonate; SRB, sulforhodamine B cell growth inhibition assay; Tf<sub>2</sub>O, trifluoromethanesulfonic anhydride

## REFERENCES

- (1) Wade, M.; Li, Y. C.; Wahl, G. M. MDM2, MDMX and p53 in oncogenesis and cancer therapy. *Nat. Rev. Cancer* **2013**, *13*, 83–96.
- (2) Vousden, K. H.; Lu, X. Live or let die: the cell's response to p53. *Nat. Rev. Cancer* **2002**, *2*, 594–604.
- (3) Stiewe, T. The p53 family in differentiation and tumorigenesis. *Nat. Rev. Cancer* **2007**, *7*, 165–168.
- (4) Toledo, F.; Wahl, G. M. Regulating the p53 pathway: in vitro hypotheses, in vivo veritas. *Nat. Rev. Cancer* **2006**, *6*, 909–923.
- (5) Brown, C. J.; Lain, S.; Verma, C. S.; Fersht, A. R.; Lane, D. P. Awakening guardian angels: drugging the p53 pathway. *Nat. Rev. Cancer* **2009**, *9*, 862–873.
- (6) Kemp, C. J.; Donehower, L. A.; Bradley, A.; Balmain, A. Reduction of p53 gene dosage does not increase initiation or promotion but enhances malignant progression of chemically induced skin tumors. *Cell* **1993**, *74*, 813–822.
- (7) Feki, A.; Irminger-Finger, I. Mutational spectrum of p53 mutations in primary breast and ovarian tumors. *Crit. Rev. Oncol. Hematol.* **2004**, *52*, 103–116.

- (8) Jones, S. N.; Roe, A. E.; Donehower, L. A.; Bradley, A. Rescue of embryonic lethality in Mdm2-deficient mice by absence of p53. *Nature* **1995**, *378*, 206–208.
- (9) Montes de Oca Luna, R.; Wagner, D. S.; Lozano, G. Rescue of early embryonic lethality in mdm2-deficient mice by deletion of p53. *Nature* **1995**, *378*, 203–206.
- (10) Freedman, D. A.; Wu, L.; Levine, A. J. Functions of the MDM2 oncoprotein. *Cell. Mol. Life Sci.* **1999**, *55*, 96–107.
- (11) Wu, X.; Bayle, J. H.; Olson, D.; Levine, A. J. The p53-mdm2 autoregulatory feedback loop. *Genes Dev.* **1993**, *7*, 1126–1132.
- (12) Juven-Gershon, T.; Oren, M. Mdm2: the ups and downs. *Mol. Med.* **1999**, *5*, 71–83.
- (13) Ganguli, G.; Abecassis, J.; Waslylyk, B. MDM2 induces hyperplasia and premalignant lesions when expressed in the basal layer of the epidermis. *EMBO J.* **2000**, *19*, 5135–5147.
- (14) Momand, J.; Jung, D.; Wilczynski, S.; Niland, J. The MDM2 gene amplification database. *Nucleic Acids Res.* **1998**, *26*, 3453–3459.
- (15) Bond, G. L.; Hu, W.; Bond, E. E.; Robins, H.; Lutzker, S. G.; Arva, N. C.; Bargoniotti, J.; Bartel, F.; Taubert, H.; Wuerl, P.; Onel, K.; Yip, L.; Hwang, S. J.; Strong, L. C.; Lozano, G.; Levine, A. J. A single nucleotide polymorphism in the MDM2 promoter attenuates the p53 tumor suppressor pathway and accelerates tumor formation in humans. *Cell* **2004**, *119*, 591–602.
- (16) Bond, G. L.; Hu, W.; Levine, A. J. MDM2 is a central node in the p53 pathway: 12 years and counting. *Curr. Cancer Drug Targets* **2005**, *5*, 3–8.
- (17) Capoulade, C.; Bressac-de Paillerets, B.; Lefrere, I.; Ronsin, M.; Feunteun, J.; Tursz, T.; Wiels, J. Overexpression of MDM2, due to enhanced translation, results in inactivation of wild-type p53 in Burkitt's lymphoma cells. *Oncogene* **1998**, *16*, 1603–1610.
- (18) Momand, J.; Wu, H. H.; Dasgupta, G. MDM2—master regulator of the p53 tumor suppressor protein. *Gene* **2000**, *242*, 15–29.
- (19) Shvarts, A.; Steegenga, W. T.; Riteco, N.; vanLaar, T.; Dekker, P.; Bazuine, M.; vanHam, R. C. A.; vanOordt, W. V.; Hateboer, G.; vanderEb, A. J.; Jochemsen, A. G. MDMX: a novel p53-binding protein with some functional properties of MDM2. *EMBO J.* **1996**, *15*, 5349–5357.
- (20) Oliner, J. D.; Kinzler, K. W.; Meltzer, P. S.; George, D. L.; Vogelstein, B. Amplification of a gene encoding a p53-associated protein in human sarcomas. *Nature* **1992**, *358*, 80–83.
- (21) Kussie, P. H.; Gorina, S.; Marechal, V.; Elenbaas, B.; Moreau, J.; Levine, A. J.; Pavletich, N. P. Structure of the MDM2 oncoprotein bound to the p53 tumor suppressor transactivation domain. *Science* **1996**, *274*, 948–953.
- (22) Riedinger, C.; McDonnell, J. M. Inhibitors of MDM2 and MDMX: a structural perspective. *Future Med. Chem.* **2009**, *1*, 1075–1094.
- (23) Millard, M.; Pathania, D.; Grande, F.; Xu, S.; Neamati, N. Small-molecule inhibitors of p53-MDM2 interaction: the 2006–2010 update. *Curr. Pharm. Des.* **2011**, *17*, 536–559.
- (24) Vassilev, L. T. MDM2 inhibitors for cancer therapy. *Trends Mol. Med.* **2007**, *13*, 23–31.
- (25) Khoury, K.; Popowicz, G. M.; Holak, T. A.; Domling, A. The p53-MDM2/MDMX axis—a chemotype perspective. *MedChemComm* **2011**, *2*, 246–260.
- (26) Wang, S.; Zhao, Y.; Bernard, D.; Aguilar, A.; Kumar, S. Targeting the MDM2-p53 protein-protein interaction for new cancer therapeutics. *Top Med. Chem.* **2012**, *8*, 57–80.
- (27) Lane, D. P.; Cheok, C. F.; Lain, S. p53-based cancer therapy. *Cold Spring Harbor Perspect. Biol.* **2010**, *2*, a001222.
- (28) Popowicz, G. M.; Domling, A.; Holak, T. A. The structure-based design of Mdm2/Mdmx-p53 inhibitors gets serious. *Angew. Chem., Int. Ed.* **2011**, *50*, 2680–2688.
- (29) Dickens, M. P.; Fitzgerald, R.; Fischer, P. M. Small-molecule inhibitors of MDM2 as new anticancer therapeutics. *Semin. Cancer Biol.* **2010**, *20*, 10–18.
- (30) Hoe, K. K.; Verma, C. S.; Lane, D. P. Drugging the p53 pathway: understanding the route to clinical efficacy. *Nat. Rev. Drug Discovery* **2014**, *13*, 217–236.
- (31) ClinicalTrials.gov identifiers for RG7112: NCT00559533, NCT00623870, NCT01677780, NCT01164033, NCT01605526, NCT01143740, and NCT01635296.
- (32) Vu, B.; Wovkulich, P.; Pizzolato, G.; Lovey, A.; Ding, Q.; Jiang, N.; Liu, J.-J.; Zhao, C.; Glenn, K.; Wen, Y.; Tovar, C.; Packman, K.; Vassilev, L.; Graves, B. Discovery of RG7112: a small-molecule MDM2 inhibitor in clinical development. *ACS Med. Chem. Lett.* **2013**, *4*, 466–469.
- (33) Ding, Q.; Zhang, Z.; Liu, J.-J.; Jiang, N.; Zhang, J.; Ross, T. M.; Chu, X.-J.; Bartkovitz, D.; Podlaski, F.; Janson, C.; Tovar, C.; Filipovic, Z. M.; Higgins, B.; Glenn, K.; Packman, K.; Vassilev, L. T.; Graves, B. Discovery of RG7388, a potent and selective p53–MDM2 inhibitor in clinical development. *J. Med. Chem.* **2013**, *56*, 5979–5983.
- (34) Siu, L. L.; Italiano, A.; Miller, W. H., Jr; Blay, J. Y.; Gietema, J. A.; Bang, Y. J.; Mileskin, L. R.; Hirte, H. W.; Reckner, M.; Higgins, B.; Jukofsky, L.; Blotner, S.; Zhi, J.; Middleton, S.; Nichols, G. L.; Chen, L. C. Phase 1 dose escalation, food effect, and biomarker study of RG7388, a more potent second-generation MDM2 antagonist, in patients (pts) with solid tumors. *J. Clin. Oncol.* **2014**, *32* (Suppl.), 2535.
- (35) ClinicalTrials.gov identifiers for MI-77301/SAR405838: NCT01636479 and NCT01985191.
- (36) Wang, S.; Sun, W.; Zhao, Y.; McEachern, D.; Meaux, I.; Barrière, C.; Stuckey, J.; Meagher, J.; Bai, B.; Liu, L.; Hoffman-Luca, C. G.; Lu, J.; Shangary, S.; Yu, S. H.; Bernard, D.; Aguilar, A.; Dos-Santos, O.; Besret, L.; Guerif, S.; Pannier, P.; Gorge-Bernat, D.; Debussche, L. SAR405838: an optimized inhibitor of MDM2-p53 interaction that induces complete and durable tumor regression. *Cancer Res.* **2014**, *74*, 5855–5865.
- (37) ClinicalTrials.gov identifiers for AMG 232: NCT01723020 and NCT02016729.
- (38) Sun, D.; Li, Z.; Rew, Y.; Gribble, M.; Bartberger, M. D.; Beck, H. P.; Canon, J.; Chen, A.; Chen, X.; Chow, D.; Deignan, J.; Duquette, J.; Eksterowicz, J.; Fisher, B.; Fox, B. M.; Fu, J.; Gonzalez, A. Z.; Gonzalez-Lopez De Turiso, F.; Houze, J. B.; Huang, X.; Jiang, M.; Jin, L.; Kayser, F.; Liu, J.; Lo, M.-C.; Long, A. M.; Lucas, B.; McGee, L. R.; McIntosh, J.; Mihalic, J.; Oliner, J. D.; Osgood, T.; Peterson, M. L.; Roveto, P.; Saiki, A. Y.; Shaffer, P.; Toteva, M.; Wang, Y.; Wang, Y. C.; Wortman, S.; Yakowec, P.; Yan, X.; Ye, Q.; Yu, D.; Yu, M.; Zhao, X.; Zhou, J.; Zhu, J.; Olson, S. H.; Medina, J. C. Discovery of AMG 232, a potent, selective, and orally bioavailable MDM2–p53 Inhibitor in clinical development. *J. Med. Chem.* **2014**, *57*, 1454–1472.
- (39) Vassilev, L. T.; Vu, B. T.; Graves, B.; Carvaljao, D.; Podlaski, F.; Filipovic, Z.; Kong, N.; Kammlott, U.; Lukacs, C.; Klein, C.; Fotouhi, N.; Liu, E. A. In vivo activation of the p53 pathway by small-molecule antagonists of MDM2. *Science* **2004**, *303*, 844–848.
- (40) Ray-Coquard, I.; Blay, J. Y.; Italiano, A.; Le Cesne, A.; Penel, N.; Zhi, J.; Heil, F.; Rueger, R.; Graves, B.; Ding, M.; Geho, D.; Middleton, S. A.; Vassilev, L. T.; Nichols, G. L.; Bui, B. N. Effect of the MDM2 antagonist RG7112 on the P53 pathway in patients with MDM2-amplified, well-differentiated or dedifferentiated liposarcoma: an exploratory proof-of-mechanism study. *Lancet Oncol.* **2012**, *13*, 1133–1140.
- (41) Shangary, S.; Qin, D.; McEachern, D.; Liu, M.; Miller, R. S.; Qiu, S.; Nikolovska-Coleska, Z.; Ding, K.; Wang, G.; Chen, J.; Bernard, D.; Zhang, J.; Lu, Y.; Gu, Q.; Shah, R. B.; Pienta, K. J.; Ling, X.; Kang, S.; Guo, M.; Sun, Y.; Yang, D.; Wang, S. Temporal activation of p53 by a specific MDM2 inhibitor is selectively toxic to tumors and leads to complete tumor growth inhibition. *Proc. Natl. Acad. Sci. U.S.A.* **2008**, *105*, 3933–3938.
- (42) ClinicalTrials.gov identifier for RG7388: NCT01773408, NCT01462175, and NCT01901172.
- (43) Ding, K.; Lu, Y.; Nikolovska-Coleska, Z.; Qiu, S.; Ding, Y. S.; Gao, W.; Stuckey, J.; Krajewski, K.; Roller, P. P.; Tomita, Y.; Parrish, D. A.; Deschamps, J. R.; Wang, S. M. Structure-based design of potent non-peptide MDM2 inhibitors. *J. Am. Chem. Soc.* **2005**, *127*, 10130–10131.

- (44) Zhao, Y.; Yu, S.; Sun, W.; Liu, L.; Lu, J.; McEachern, D.; Shargary, S.; Bernard, D.; Li, X.; Zhao, T.; Zou, P.; Sun, D.; Wang, S. A potent small-molecule inhibitor of the MDM2–p53 interaction (MI-888) achieved complete and durable tumor regression in mice. *J. Med. Chem.* **2013**, *56*, 5553–5561.
- (45) Yu, S. H.; Qin, D. G.; Shargary, S.; Chen, J. Y.; Wang, G. P.; Ding, K.; McEachern, D.; Qiu, S.; Nikolovska-Coleska, Z.; Miller, R.; Kang, S. M.; Yang, D. J.; Wang, S. M. Potent and orally active small-molecule inhibitors of the MDM2-p53 interaction. *J. Med. Chem.* **2009**, *52*, 7970–7973.
- (46) Carry, J.-C.; Garcia-Echeverria, C. Inhibitors of the p53/Hdm2 protein–protein interaction—path to the clinic. *Bioorg. Med. Chem. Lett.* **2013**, *23*, 2480–2485.
- (47) Wang, S.; Zhao, Y.; Sun, W.; Kumar, S.; Leopold, L.; Debussche, L.; Barriere, C.; Carry, J. C.; Amaning, K. Spiro-oxindole MDM2 antagonists. PCT Patent Publication Number WO 2012/06022 A2, 2012.
- (48) Rew, Y.; Sun, D. Q.; De Turiso, F. G. L.; Bartberger, M. D.; Beck, H. P.; Canon, J.; Chen, A.; Chow, D.; Deignan, J.; Fox, B. M.; Gustin, D.; Huang, X.; Jiang, M.; Jiao, X. Y.; Jin, L. X.; Kayser, F.; Kopecky, D. J.; Li, Y. H.; Lo, M. C.; Long, A. M.; Michelsen, K.; Oliner, J. D.; Osgood, T.; Ragains, M.; Saiki, A. Y.; Schneider, S.; Toteva, M.; Yakowec, P.; Yan, X. L.; Ye, Q. P.; Yu, D. Y.; Zhao, X. N.; Zhou, J.; Medina, J. C.; Olson, S. H. Structure-based design of novel inhibitors of the MDM2-p53 interaction. *J. Med. Chem.* **2012**, *55*, 4936–4954.
- (49) Michelsen, K.; Jordan, J. B.; Lewis, J.; Long, A. M.; Yang, E.; Rew, Y.; Zhou, J.; Yakowec, P.; Schnier, P. D.; Huang, X.; Poppe, L. Ordering of the N-terminus of human MDM2 by small molecule inhibitors. *J. Am. Chem. Soc.* **2012**, *134*, 17059–17067.
- (50) Lucas, B. S.; Fisher, B.; McGee, L. R.; Olson, S. H.; Medina, J. C.; Cheung, E. An expeditious synthesis of the MDM2–p53 inhibitor AM-8553. *J. Am. Chem. Soc.* **2012**, *134*, 12855–12860.
- (51) Perez-Moreno, P.; Brambilla, E.; Thomas, R.; Soria, J. C. Squamous cell carcinoma of the lung: molecular subtypes and therapeutic opportunities. *Clin. Cancer Res.* **2012**, *18*, 2443–2451.
- (52) Raboisson, P.; Marugan, J. J.; Schubert, C.; Koblish, H. K.; Lu, T.; Zhao, S.; Player, M. R.; Maroney, A. C.; Reed, R. L.; Huebert, N. D.; Lattanzi, J.; Parks, D. J.; Cummings, M. D. Structure-based design, synthesis, and biological evaluation of novel 1,4-diazepines as HDM2 antagonists. *Bioorg. Med. Chem. Lett.* **2005**, *15*, 1857–1861.
- (53) Parks, D. J.; LaFrance, L. V.; Calvo, R. R.; Milkiewicz, K. L.; Marugan, J. J.; Raboisson, P.; Schubert, C.; Koblish, H. K.; Zhao, S.; Franks, C. F.; Lattanzi, J.; Carver, T. E.; Cummings, M. D.; Maguire, D.; Grasberger, B. L.; Maroney, A. C.; Lu, T. Enhanced pharmacokinetic properties of 1,4-benzodiazepine-2,5-dione antagonists of the HDM2-p53 protein–protein interaction through structure-based drug design. *Bioorg. Med. Chem. Lett.* **2006**, *16*, 3310–3314.
- (54) Grasberger, B. L.; Lu, T.; Schubert, C.; Parks, D. J.; Carver, T. E.; Koblish, H. K.; Cummings, M. D.; LaFrance, L. V.; Milkiewicz, K. L.; Calvo, R. R.; Maguire, D.; Lattanzi, J.; Franks, C. F.; Zhao, S.; Ramachandren, K.; Bylebyl, G. R.; Zhang, M.; Manthey, C. L.; Petrella, E. C.; Pantoliano, M. W.; Deckman, I. C.; Spurlino, J. C.; Maroney, A. C.; Tomczuk, B. E.; Molloy, C. J.; Bone, R. F. Discovery and cocrystal structure of benzodiazepinedione HDM2 antagonists that activate p53 in cells. *J. Med. Chem.* **2005**, *48*, 909–912.
- (55) Marugan, J. J.; Leonard, K.; Raboisson, P.; Gushue, J. M.; Calvo, R.; Koblish, H. K.; Lattanzi, J.; Zhao, S.; Cummings, M. D.; Player, M. R.; Schubert, C.; Maroney, A. C.; Lu, T. Enantiomerically pure 1,4-benzodiazepine-2,5-diones as Hdm2 antagonists. *Bioorg. Med. Chem. Lett.* **2006**, *16*, 3115–3120.
- (56) Hardcastle, I. R.; Liu, J. F.; Valeur, E.; Watson, A.; Ahmed, S. U.; Blackburn, T. J.; Bennaceur, K.; Clegg, W.; Drummond, C.; Endicott, J. A.; Golding, B. T.; Griffin, R. J.; Gruber, J.; Haggerty, K.; Harrington, R. W.; Hutton, C.; Kemp, S.; Lu, X. C.; McDonnell, J. M.; Newell, D. R.; Noble, M. E. M.; Payne, S. L.; Revill, C. H.; Riedinger, C.; Xu, Q.; Lunec, J. Isoindolinone inhibitors of the murine double minute 2 (MDM2)-p53 protein–protein interaction: structure–activity studies leading to improved potency. *J. Med. Chem.* **2011**, *54*, 1233–1243.
- (57) Beck, H. P.; DeGraffenreid, M.; Fox, B.; Allen, J. G.; Rew, Y.; Schneider, S.; Saiki, A. Y.; Yu, D.; Oliner, J. D.; Salyers, K.; Ye, Q.; Olson, S. Improvement of the synthesis and pharmacokinetic properties of chromenotriazolopyrimidine MDM2-p53 protein–protein inhibitors. *Bioorg. Med. Chem. Lett.* **2011**, *21*, 2752–2755.
- (58) Bertamino, A.; Soprano, M.; Musella, S.; Rusciano, M. R.; Sala, M.; Vernieri, E.; Di Sarno, V.; Limatola, A.; Carotenuto, A.; Cosconati, S.; Grieco, P.; Novellino, E.; Illario, M.; Campiglia, P.; Gomez-Monterrey, I. Synthesis, in vitro, and in cell studies of a new series of [indoline-3,2'-thiazolidine]-based p53 modulators. *J. Med. Chem.* **2013**, *56*, 5407–5421.
- (59) Miyazaki, M.; Naito, H.; Sugimoto, Y.; Yoshida, K.; Kawato, H.; Okayama, T.; Shimizu, H.; Kitagawa, M.; Seki, T.; Fukutake, S.; Shiose, Y.; Aonuma, M.; Soga, T. Synthesis and evaluation of novel orally active p53-MDM2 interaction inhibitors. *Bioorg. Med. Chem.* **2013**, *21*, 4319–4331.
- (60) Furet, P.; Chene, P.; De Pover, A.; Valat, T. S.; Lisztwan, J. H.; Kallen, J.; Masuya, K. The central valine concept provides an entry in a new class of non peptide inhibitors of the p53-MDM2 interaction. *Bioorg. Med. Chem. Lett.* **2012**, *22*, 3498–3502.
- (61) Czarna, A.; Beck, B.; Srivastava, S.; Popowicz, G. M.; Wolf, S.; Huang, Y.; Bista, M.; Holak, T. A.; Domling, A. Robust generation of lead compounds for protein–protein interactions by computational and MCR chemistry: p53/Hdm2 antagonists. *Angew. Chem., Int. Ed.* **2010**, *49*, 5352–5356.
- (62) Huang, Y.; Wolf, S.; Koes, D.; Popowicz, G. M.; Camacho, C. J.; Holak, T. A.; Domling, A. Exhaustive fluorine scanning toward potent p53-Mdm2 antagonists. *ChemMedChem* **2012**, *7*, 49–52.
- (63) Zhuang, C.; Miao, Z.; Zhu, L.; Dong, G.; Guo, Z.; Wang, S.; Zhang, Y.; Wu, Y.; Yao, J.; Sheng, C.; Zhang, W. Discovery, synthesis, and biological evaluation of orally active pyrrolidone derivatives as novel inhibitors of p53–MDM2 protein–protein interaction. *J. Med. Chem.* **2012**, *55*, 9630–9642.
- (64) Wang, W. S.; Zhu, X. L.; Hong, X. Q.; Zheng, L.; Zhu, H.; Hu, Y. Z. Identification of novel inhibitors of p53-MDM2 interaction facilitated by pharmacophore-based virtual screening combining molecular docking strategy. *MedChemComm* **2013**, *4*, 411–416.
- (65) Ma, Y.; Lahue, B. R.; Gibeau, C. R.; Shipps, G. W., Jr.; Bogen, S. L.; Wang, Y.; Guo, Z.; Guzi, T. J. Pivotal role of an aliphatic side chain in the development of an HDM2 inhibitor. *ACS Med. Chem. Lett.* **2014**, *5*, 572–575.
- (66) Pan, W.; Lahue, B. R.; Ma, Y.; Nair, L. G.; Shipps, G. W., Jr.; Wang, Y.; Doll, R.; Bogen, S. L. Core modification of substituted piperidines as novel inhibitors of HDM2–p53 protein–protein interaction. *Bioorg. Med. Chem. Lett.* **2014**, *24*, 1983–1986.
- (67) Gonzalez, A. Z.; Eksterowicz, J.; Bartberger, M. D.; Beck, H. P.; Canon, J.; Chen, A.; Chow, D.; Duquette, J.; Fox, B. M.; Fu, J.; Huang, X.; Houze, J. B.; Jin, L.; Li, Y.; Li, Z.; Ling, Y.; Lo, M.-C.; Long, A. M.; McGee, L. R.; McIntosh, J.; McMinn, D. L.; Oliner, J. D.; Osgood, T.; Rew, Y.; Saiki, A. Y.; Shaffer, P.; Wortman, S.; Yakowec, P.; Yan, X.; Ye, Q.; Yu, D.; Zhao, X.; Zhou, J.; Olson, S. H.; Medina, J. C.; Sun, D. Selective and potent morpholinone inhibitors of the MDM2–p53 protein–protein interaction. *J. Med. Chem.* **2014**, *57*, 2472–2488.
- (68) Gonzalez, A. Z.; Li, Z.; Beck, H. P.; Canon, J.; Chen, A.; Chow, D.; Duquette, J.; Eksterowicz, J.; Fox, B. M.; Fu, J.; Huang, X.; Houze, J.; Jin, L.; Li, Y.; Ling, Y.; Lo, M.-C.; Long, A. M.; McGee, L. R.; McIntosh, J.; Oliner, J. D.; Osgood, T.; Rew, Y.; Saiki, A. Y.; Shaffer, P.; Wortman, S.; Yakowec, P.; Yan, X.; Ye, Q.; Yu, D.; Zhao, X.; Zhou, J.; Olson, S. H.; Sun, D.; Medina, J. C. Novel inhibitors of the MDM2-p53 interaction featuring hydrogen bond acceptors as carboxylic acid isosteres. *J. Med. Chem.* **2014**, *57*, 2963–2988.
- (69) Zhang, Z.; Chu, X.-J.; Liu, J.-J.; Ding, Q.; Zhang, J.; Bartkovitz, D.; Jiang, N.; Karnachi, P.; So, S.-S.; Tovar, C.; Filipovic, Z. M.; Higgins, B.; Glenn, K.; Packman, K.; Vassilev, L.; Graves, B. Discovery of potent and orally active p53-MDM2 inhibitors RO5353 and RO2468 for potential clinical development. *ACS Med. Chem. Lett.* **2013**, *5*, 124–127.
- (70) Hardcastle, I. R.; Ahmed, S. U.; Atkins, H.; Farnie, G.; Golding, B. T.; Griffin, R. J.; Guyenne, S.; Hutton, C.; Kallblad, P.; Kemp, S. J.

Kitching, M. S.; Newell, D. R.; Norbedo, S.; Northen, J. S.; Reid, R. J.; Saravanan, K.; Willems, H. M.; Lunec, J. Small-molecule inhibitors of the MDM2-p53 protein–protein interaction based on an isoindolinone scaffold. *J. Med. Chem.* **2006**, *49*, 6209–6221.

(71) Hardcastle, I. R.; Ahmed, S. U.; Atkins, H.; Calvert, A. H.; Curtin, N. J.; Farnie, G.; Golding, B. T.; Griffin, R. J.; Guyenne, S.; Hutton, C.; Kallblad, P.; Kemp, S. J.; Kitching, M. S.; Newell, D. R.; Norbedo, S.; Northen, J. S.; Reid, R. J.; Saravanan, K.; Willems, H. M.; Lunec, J. Isoindolinone-based inhibitors of the MDM2-p53 protein–protein interaction. *Bioorg. Med. Chem. Lett.* **2005**, *15*, 1515–1520.

(72) Allen, J. G.; Bourbeau, M. P.; Wohlhieter, G. E.; Bartberger, M. D.; Michelsen, K.; Hungate, R.; Gadwood, R. C.; Gaston, R. D.; Evans, B.; Mann, L. W.; Matison, M. E.; Schneider, S.; Huang, X.; Yu, D.; Andrews, P. S.; Reichelt, A.; Long, A. M.; Yakowec, P.; Yang, E. Y.; Lee, T. A.; Oliner, J. D. Discovery and optimization of chromenotriazolopyrimidines as potent inhibitors of the mouse double minute 2–tumor protein 53 protein–protein interaction. *J. Med. Chem.* **2009**, *52*, 7044–7053.

(73) Gomez-Monterrey, I.; Bertamino, A.; Porta, A.; Carotenuto, A.; Musella, S.; Aquino, C.; Granata, I.; Sala, M.; Brancaccio, D.; Picone, D.; Ercole, C.; Stiuso, P.; Campiglia, P.; Grieco, P.; Ianelli, P.; Maresca, B.; Novellino, E. Identification of the spiro(oxindole-3,3'-thiazolidine)-based derivatives as potential p53 activity modulators. *J. Med. Chem.* **2010**, *53*, 8319–8329.

(74) Popowicz, G. M.; Czarna, A.; Wolf, S.; Wang, K.; Wang, W.; Domling, A.; Holak, T. A. Structures of low molecular weight inhibitors bound to MDMX and MDM2 reveal new approaches for p53-MDMX/MDM2 antagonist drug discovery. *Cell Cycle* **2010**, *9*, 1104–1111.

(75) Ma, Y.; Lahue, B. R.; Shipps, G. W.; Brookes, J.; Wang, Y. L. Substituted piperidines as HDM2 inhibitors. *Bioorg. Med. Chem. Lett.* **2014**, *24*, 1026–1030.

(76) El-Deiry, W. S.; Tokino, T.; Velculescu, V. E.; Levy, D. B.; Parsons, R.; Trent, J. M.; Lin, D.; Mercer, W. E.; Kinzler, K. W.; Vogelstein, B. WAF1, a potential mediator of p53 tumor suppression. *Cell* **1993**, *75*, 817–825.

(77) Nakano, K.; Vousden, K. H. PUMA, a novel proapoptotic gene, is induced by p53. *Mol. Cell* **2001**, *7*, 683–694.

(78) Tovar, C.; Rosinski, J.; Filipovic, Z.; Higgins, B.; Kolinsky, K.; Hilton, H.; Zhao, X.; Vu, B. T.; Qing, W.; Packman, K.; Myklebost, O.; Heimbrook, D. C.; Vassilev, L. T. Small-molecule MDM2 antagonists reveal aberrant p53 signaling in cancer: implications for therapy. *Proc. Natl. Acad. Sci. U.S.A.* **2006**, *103*, 1888–1893.

(79) Weaver, J.; Downs-Kelly, E.; Goldblum, J. R.; Turner, S.; Kulkarni, S.; Tubbs, R. R.; Rubin, B. P.; Skacel, M. Fluorescence in situ hybridization for MDM2 gene amplification as a diagnostic tool in lipomatous neoplasms. *Mod. Pathol.* **2008**, *21*, 943–949.

(80) Weaver, J.; Goldblum, J. R.; Turner, S.; Tubbs, R. R.; Wang, W. L.; Lazar, A. J.; Rubin, B. P. Detection of MDM2 gene amplification or protein expression distinguishes sclerosing mesenteritis and retroperitoneal fibrosis from inflammatory well-differentiated liposarcoma. *Mod. Pathol.* **2009**, *22*, 66–70.

(81) Gilkes, D. M.; Pan, Y.; Coppola, D.; Yeatman, T.; Reuther, G. W.; Chen, J. Regulation of MDMX expression by mitogenic signaling. *Mol. Cell. Biol.* **2008**, *28*, 1999–2010.

(82) Aziz, M. H.; Shen, H.; Maki, C. G. Acquisition of p53 mutations in response to the non-genotoxic p53 activator Nutlin-3. *Oncogene* **2011**, *30*, 4678–4686.

(83) Iancu-Rubin, C.; Mosoyan, G.; Glenn, K.; Gordon, R. E.; Nichols, G. L.; Hoffman, R. Activation of p53 by the MDM2 inhibitor RG7112 impairs thrombopoiesis. *Exp. Hematol.* **2014**, *42*, 137–45 e5.